

NKS-447  
ISBN 978-87-7893-539-7

---

Corrosion of copper in sulphide containing environment:  
the role and properties of sulphide films –  
Annual report 2020

Elisa Isotahdon<sup>1</sup>, Vilma Ratia<sup>1</sup>, Pauliina Rajala<sup>1</sup>, Leena Carpén<sup>1</sup>

Cem Örnek<sup>2</sup>, Fan Zhang<sup>2</sup>, Jinshan Pan<sup>2</sup>

<sup>1</sup>VTT Technical Research Centre of Finland Ltd., Espoo, Finland

<sup>2</sup>KTH Royal Institute of Technology, Stockholm, Sweden

April 2021

## **Abstract**

In COCOS project, the role and properties of sulphide films on copper surface are studied. OFP-copper samples were exposed to sulfide-containing anoxic simulated groundwater for different durations. In 2020, the second year of the COCOS project, the work continued with characterization of previously exposed OFP-copper samples by new techniques. Also, new 9-month long exposure tests were started with sulphide concentrations ranging from 0 to 320 mg/L.

The electrochemical measurements were conducted across the duration of the exposure test. As a result, trends in corrosion behaviour of copper was seen throughout the test. EIS results indicated the formation of the different corrosion product films on sample surfaces exposed. The protective effect of surface layers changes with time of exposure, and the behaviour is influenced by the amount of sulphide in the environment. A distinct and sharp increases in the open circuit potential values of copper samples were observed in some cases during the test. These were more common in environments with low sulphide amount and may be related to time when sulphide has been consumed by chemical reactions. The observation will be further studied in future.

Corrosion rate of samples exposed to 0 mg/L, 32 mg/L and 320 mg/L of sulphide was determined also by measuring mass loss during 4-month test. One interesting finding was that the highest corrosion rates, ca. 0.4  $\mu\text{m/a}$ , were obtained for samples exposed to sulphide content of 32 mg/L. Sample characterisation showed that the highest mass loss was most likely due to local defects on the samples, not uniform corrosion.

HEXRD studies revealed significant lattice changes as deformation extending several hundreds of micrometers into the bulk. This is attributed to H infusion. The results demonstrate the risk for H-induced stress corrosion cracking of copper as canister material during long-term storage of nuclear fuel when exposed to sulfide-containing groundwater.

The last year of the project is going on at the moment. Longer term experiments have been performed. Further analysis of new samples and data from electrochemical measurements from longer exposures continues. Also, the last new experimental tests will be conducted in 2021.

## **Key words**

corrosion, copper, nuclear waste, sulphide, characterisation

NKS-447  
ISBN 978-87-7893-539-7  
Electronic report, April 2021  
NKS Secretariat  
P.O. Box 49  
DK - 4000 Roskilde, Denmark  
Phone +45 4677 4041  
[www.nks.org](http://www.nks.org)  
e-mail [nks@nks.org](mailto:nks@nks.org)

# **Corrosion of copper in sulphide containing environment: the role and properties of sulphide films - Annual report 2020**

**Second annual report from the NKS-R COCOS (Contract: AFT/NKS-  
R(20)127/2)**

Elisa Isotahdon<sup>1</sup>, Vilma Ratia<sup>1</sup>, Pauliina Rajala<sup>1</sup>, Leena Carpén<sup>1</sup>,  
Cem Örneke<sup>2</sup>, Fan Zhang<sup>2</sup>, Jinshan Pan<sup>2</sup>

<sup>1</sup>VTT Technical Research Centre of Finland Ltd., Espoo, Finland

<sup>2</sup>KTH Royal Institute of Technology, Stockholm, Sweden

## Table of contents

1. Introduction .....	3
2. Scope of the project.....	4
3. Materials and methods .....	5
3.1 Materials.....	5
3.2 Exposure conditions and experiments conducted in 2020 .....	5
3.3 Methods.....	6
3.3.1 Electrochemical methods .....	6
3.3.2 Mass loss determination .....	7
3.3.3 Microscopy.....	7
3.3.4 Water chemistry measurements .....	7
3.3.5 Raman spectroscopy.....	8
3.3.6 Grazing incidence angle x-ray diffraction (GIXRD) .....	8
3.3.7 Synchrotron High-energy X-ray diffraction (HEXRD) .....	8
3.3.8 Scanning Kelvin probe force microscopy (SKPFM) .....	8
3.3.9 Additional test for glass-sulphide interactions .....	9
4. Results and discussion.....	10
4.1 Corrosion measurements .....	10
4.1.1 Electrochemical measurements (Test initiated in 2019) .....	10
4.1.2 Electrochemical measurements (8- and 9-month tests).....	14
4.1.3. Corrosion rate and mass loss (4-month experiment).....	16
4.2 More detailed surface characterisation of samples from experiments initiated in 2019 ....	18
4.2.1 SEM EDS study of the surfaces of electrochemical samples.....	18
4.2.2 GIXRD and Raman studies .....	23
4.2.3. Synchrotron HEXRD results and DFT calculation .....	26
4.2.4. SKPFM results .....	28
4.3 Additional experimental tests.....	30
4.3.1. Glass corrosion related to experimental test .....	30
4.3.2 Microstructure of copper samples used.....	32
5. Summary and conclusions.....	34

## 1. Introduction

This is the second annual report for project COCOS. The aim of the project is to characterise the role and properties of sulphide films on copper corrosion. This report covers the activities performed during 2020, the second year of this three-year project.

The nuclear waste disposal concept in Finland and in Sweden is based on a multi-barrier system (King et al., 2013, Salonen et al., 2021). The spent nuclear fuel will be placed in cast iron containers, which are sealed inside of copper canisters. Copper canisters are further placed in the holes drilled into deep bedrock. Canisters are surrounded with compacted bentonite clay that forms buffer around copper canisters. Bentonite buffer is believed to provide a favorable environment, where the integrity of copper canisters should retain at least 100 000 years. The repository conditions are believed to transform to anoxic rapidly after closure of repository (Nuclear Waste State of the Art Report 2011, 2011).

Copper was chosen to serve as a corrosion barrier for the disposal canister because of its assumed resistance to corrosion under anoxic conditions. The disposal canister plays a major part of the multi-barrier concept. Possible failure mechanisms endangering the reliability of the copper canister have been assessed by models based on literature, corrosion tests simulating the disposal conditions and copper items found in nature (King et al., 2010).

The most severe failure mechanisms of outer copper canisters have been evaluated and copper-sulfide interactions have been identified as one of the possible failure mechanisms (Huttunen-Saarivirta et al., 2018; Salonen et al., 2021). Bentonite buffer might be source of sulfide, but most importantly sulfide is expected to be formed from sulphate in microbial process called sulphate reduction (Huttunen-Saarivirta et al., 2017). Sulphate is abundant in ground water at disposal site and it can also be released through cation exchange mechanisms from bentonite buffer. Bacteria capable of reduction sulphate to sulfide are native to the groundwater at the repository site (Huttunen-Saarivirta et al., 2017). Sulfide can cause failure of copper canister by inducing general corrosion of copper (Salonen et al., 2021). Moreover, uniform copper-sulfide film could protect the canister from corrosion in certain conditions. In event of formation of protective  $\text{Cu}_2\text{S}$  film, it is possible that the localized rupture of protective film could induce localized corrosion (Huttunen-Saarivirta et al., 2018). Indeed, the complex role and behaviour of sulphide films on copper surface give motivation for detailed study on this subject.

Work in this project is a collaboration between VTT Technical Research Centre of Finland Ltd. and KTH Royal Institute of Technology, Sweden. The first annual report, NKS-434 (Ratia et al., 2020), summarized the research background and contained a review section regarding the studied phenomena. A short summary of our scope is given in chapter 2.

## 2. Scope of the project

Corrosion of copper under oxic and anoxic conditions, and microbiologically-influenced corrosion, have been intensively investigated over 40 years. A recent review gives an overview of the corrosion issues, debated questions, and ongoing research programs (Hall et al., 2021). A number of SKB reports assessing corrosion of copper canister under expected repository conditions have concluded that there is no considerable risk for canister failure. However, the risks for several complex forms of copper corrosion have been debated in Sweden, even in the Land and Environmental Court, leading to the statement to the Swedish Government, that supplementary information related to the long-term behaviour of the copper canisters should be presented and evaluated regarding five issues: i) corrosion due to reaction in oxygen-free water; ii) pitting due to reaction with sulphide; iii) stress corrosion cracking due to reaction with sulphide; iv) hydrogen embrittlement; v) the effect of radioactive radiation on pitting, stress corrosion cracking and hydrogen embrittlement (SKB - Svensk Kärnbränslehantering AB et al., 2019). Clearly, there is a need to gain a deep understanding of the role of sulphur and hydrogen in hydrogen embrittlement and stress corrosion cracking of copper during exposure to the ground water containing sulphide. The aim of our work is to gain such knowledge by detailed analyses of copper samples during and after the exposure to anoxic simulated groundwater containing sulphide.

### 3. Materials and methods

#### 3.1 Materials

Hot rolled oxygen-free phosphorus-containing copper (OFP-Cu) was used as the material for the experiments. OFP-Cu was provided by Posiva Oyj for research purposes. Two initial conditions were used: (i) the polished copper surface and (ii) pre-oxidised copper surface, which was exposed to 90 °C temperature in air for seven days after grinding. The pre-oxidation is applied to simulate the effect of previous exposure to oxic conditions on the copper material (prior to unoxic phase in disposal).

Three different sample types were used for different purposes. The electrochemical samples had a reactive area of 1 cm<sup>2</sup>. These samples had the surface finish of 600 grit and were tested only with as-ground surfaces (no pre-oxidized). For the mass loss measurements, coupons of approximately 70\*25\*(3-5) mm with surface finish of 600 grit, were used. For material characterisation purposes, samples with the dimensions of approximately 10\*10\*(2-5) mm with selected surfaces polished to 1 µm were used. All samples were cleaned in acetone and ethanol prior to the test.

#### 3.2 Exposure conditions and experiments conducted in 2020

All exposure experiments were conducted at VTT. The samples were exposed to simulated groundwater with varied concentrations of sulphide. The chemical components (presented in Table 1) of the simulated groundwater are modelled based on the groundwater chemistry of the planned disposal site with added effects of bentonite. The varied sulphide addition to the solution was made in form of Na<sub>2</sub>S. All the used sulphide concentrations in this project are presented in Table 2. The highest amount, 640 mg/L was used only in the first experiment initiated in 2019. The experiments were conducted at room temperature (22 °C). The test vessels for gravimetric samples and characterisation samples were gas tight laboratory glass bottles with volume of 5 L. The electrochemical samples were placed in their own bottles with volume of 2 L. The experiments were carried out in anoxic environment: water and vessels were flushed with argon before the initiating the test. Vessels were sealed with butyl rubber stoppers to prevent oxygen contamination during the experiment. Vessels with electrochemical measurement setup were purged regularly with argon during the exposure period to maintain anoxic conditions.

**Table 1.** The chemical components of the simulated groundwater.

	K	Ca	Cl	Na*	SO <sub>4</sub>	Br	HCO <sub>3</sub>	Mg	Sr	Si	B	F	Mn	PO <sub>4</sub>	lactate
mg/L	54.7	280.0	5274.0	3180.2	595.0	42.3	13.7	100.0	8.8	3.1	1.1	0.8	0.2	0.1	1

\*original Na addition; actual amount is dependent on the addition of Na<sub>2</sub>S

**Table 2.** Used sulphide additions and their corresponding concentrations.

Sulphide (S <sup>2-</sup> ) addition	Concentration of the solution
0 mg/L	0
3 mg/L	10 <sup>-4</sup> mol/L
32 mg/L	10 <sup>-3</sup> mol/L
320 mg/L	10 <sup>-2</sup> mol/L
640 mg/L	2*10 <sup>-2</sup> mol/L

In 2019, tests with planned durations of about two months (53 days, 32 mg/L S<sup>2-</sup>) and four months (135 days with 0, 3, 32, 320 and 640 mg/L S<sup>2-</sup>) were conducted and finished. Test vessels with electrochemical measurements had a duration of 8 months (256 days with 0, 32 and 320 mg/L S<sup>2-</sup>) as they were initiated in 2019 and finished in early 2020. During 2020 the analysis of samples from previously described tests continued.

In year 2020, a longer, 9-month long experiments were started with sulphide concentrations ranging from 0 to 320 mg/L. Due to the oxygen leakage in electrochemical measurements initiated in 2019, some parallel measurements were initiated in 2020 with improved setup to reduce the possibility for air and O<sub>2</sub> permeation into the test vessels.

Two of the test vessels built up in 2020, one with gravimetric samples and one with electrochemical measurements, were started with sulphide content of 3 mg/L, but Na<sub>2</sub>S additions are done intermittently during the exposure period so that in the end of test period the sulphide content is targeted to 320 mg/L. The 9-month experiment started in 2020 are terminated as planned in spring 2021.

### 3.3 Methods

#### 3.3.1 Electrochemical methods

The surface behaviour and corrosion of the samples were monitored with electrochemical measurements. Open circuit potential (OCP) and redox potential data were collected continuously throughout the experimental period. The used reference electrode was Ag/AgCl (anaerobic, 0.15 M KCl). A platinum electrode immersed in the vessels was used for redox measurements.

Linear polarization resistance (LPR), electrochemical impedance spectroscopy (EIS) and Tafel measurements were conducted once a week. Counter electrode was platinum and a copper electrode was used as a working electrode and another as a pseudo-reference electrode in these measurements. LPR measurement range was -20 to 20 mV vs. E<sub>OC</sub> with the scan rate of 0.16667 mV/s and Tafel from -30 to 30 mV vs. E<sub>OC</sub> with the scan rate of 0.16667 mV/s. The EIS was measured at OCP with 10 mV AC voltage, from 100000 to 0.001 Hz, eight points per decade. The OCP measurements were conducted for 60 s at the start of these measurements. All the electrochemical measurements were performed using a Gamry Instruments potentiostat model Reference 600<sup>TM</sup> with DC105 and EIS300 software. Gamry Echem software was used to fit the Tafel and polarisation resistance plots.

The corrosion rate was calculated from the corrosion current in two different ways. The calculation of the corrosion rate (CR) is derived from the Faraday's law and according to ASTM standard G102-89 (ASTM, 1999) is calculated as:

$$CR = (i_{\text{corr}} * K * EW) / \rho$$

where  $i_{\text{corr}}$  is corrosion current density (corrosion current  $I_{\text{corr}}$  divided by the sample area),  $K$  is a constant depending on the wanted unit of the outcome,  $EW$  equivalent weight and  $\rho$  the density of copper. For corrosion rates presented in mm/a, the constant  $K$  is 3272 mm/(A\*cm\*year) (Gamry, 2020).

In the first method, the  $I_{\text{corr}}$  is determined by using Tafel extrapolation. In the second calculation method,  $I_{\text{corr}}$  is calculated with the formula:

$$I_{\text{corr}} = (\beta_a \cdot \beta_c) / (2.303 \cdot R_p \cdot (\beta_a + \beta_c))$$

where the  $\beta$  coefficients are obtained from the Tafel plots and the polarisation resistance ( $R_p$ ) from the linear polarisation curve (Gamry, 2020).

### 3.3.2 Mass loss determination

Mass losses were determined for samples that had been exposed to test vessels with 0, 32 and 320 mg/L sulphide addition. After the exposure, loose corrosion products on sample surface were removed by pickling with a solution of 500 mL of HCl (37%), 500 mL distilled water and 3.5 g of hexamethylenetetramine ((CH<sub>2</sub>)<sub>6</sub>N<sub>4</sub>). The pickling was done 3-5 times, until a steady weight was achieved for the sample.

Based on this mass loss, the corrosion rate ( $r_{\text{corr}}$  in  $\mu\text{m/a}$ ) was calculated with the formula:

$$r_{\text{corr}} = (dm \cdot 365 \cdot 10) / (A \cdot t \cdot \rho)$$

where  $dm$  is mass loss (mg),  $A$  area (cm<sup>2</sup>),  $t$  time (d) and ( $\rho$ ) density of copper (g/cm<sup>3</sup>). The mass loss results, based on which the calculations were made, were corrected for the pickling with reference samples: similar material in untreated and pre-oxidised state was pickled and mass loss from the pickling in comparison to the original untreated mass was retracted from the results to eliminate the effects of pickling.

### 3.3.3 Microscopy

All samples were visually inspected and photographed after the exposure. The surfaces were also examined with an optical stereomicroscope Leica MZ7.5.

Scanning electron microscope with field emission gun (FEGSEM) Zeiss UltraPlus Gemini was used for characterising the surfaces after the exposure in more detail with both secondary electron (SE) and backscattered electron (BSE) modes. Moreover, energy dispersive X-ray spectroscopy (EDS) Thermoscientific UltraDry was used to obtain information on the chemical components present on the surfaces.

To study the grain size and orientation of the copper material, one sample was etched with the same pickling solution as used in mass loss determination (H<sub>2</sub>O + HCl + (CH<sub>2</sub>)<sub>6</sub>N<sub>4</sub>) and then studied with optical microscope.

### 3.3.4 Water chemistry measurements

The water chemistry measurements were conducted at ALS Finland Oy with a number of analysis methods for different components of the solution. pH, alkalinity, conductivity, acidity, carbon dioxide and carbonates were determined with potentiometric titration (EN ISO 9963-1 and CSN 75 7373); Br, F, Cl and SO<sub>4</sub> with ion chromatography (ISO 10304-1, EN 16192); hydrogen sulphide and sulphide with spectrophotometry (CSN 83 0520-16, CSN 83 0530-31, SM 4500-S D); and B, Ca, Cu, Mg, Mn, K, Na, Si, Sr with inductively coupled plasma - mass spectrometry and atomic fluorescence spectroscopy (EPA 200.8, EN ISO 17294-2, EPA 6020A, EPA 245.7, EPA 1631, EN ISO 178 52, EN 16192). In this project, the analyses were conducted to test solutions normally after the exposure test. In 2020, water analysis was used for the additional tests that were done to clarify the effects on the test solution on borosilicate glass material.

### **3.3.5 Raman spectroscopy**

Samples were studied with two Raman instruments: Kaiser Optical Systems RamanRxn2 Hybrid CW Raman excitation wavelength 875 nm and Timegate Instruments time-gated PicoRaman excitation wavelength 532 nm. Kaiser measurements were done with standard non-contact probe. Timegate measurement were done with microscope setup using 40x and 100x objectives.

### **3.3.6 Grazing incidence angle x-ray diffraction (GIXRD)**

The samples from the 4-month experiment and unexposed reference samples were analysed using a Philips x-ray diffractometer X'Pert MPD at VTT. The phase composition of the corrosion products on specimens were studied using grazing incidence angles (GIXRD) of 0.3, 0.5, 1, 2.5 and 5°. Grazing incident angle was fixed between specimen and incident beam. Cu K $\alpha$  X-ray tube operating at 45 kV and 40 mA using a step size of 0.01° and time per step of 54.57 s for XRD and 38 s were used for GIXRD.

Moreover, in January 2020, the KTH group performed synchrotron GIXRD measurements of the 4-month samples using the surface diffraction beamline I07 at Diamond Light Source in the UK. The diffracted signal was measured in grazing incidence geometry using in-plane scans with an incidence angle of 0.2° and 0.05°, respectively. The energy of the incident X-ray beam was 20.5 keV, with a beam size of 100  $\mu\text{m}$  (vertical) x 300  $\mu\text{m}$  (horizontal) at the sample position. The experiment was performed with a DECTRIS Pilatus 100K two-dimensional detector with an area of 487x195 pixels (pixel size of 172x172  $\mu\text{m}^2$ ) at a distance of 900 mm from the sample. The use of a small grazing incidence angle in X-ray diffraction experiments allows to reduce the subsurface beam penetration (more surface sensitive) to detect thin layer of corrosion products, and also permits to probe the outermost surface grains to measure the evolution of lattice strain associated with hydrogen infusion. The data analysis is still ongoing, the general observation is given here, and detailed results will be documented in the next report.

### **3.3.7 Synchrotron High-energy X-ray diffraction (HEXRD)**

In August 2019, the HEXRD measurements of three two-month samples were performed at the Swedish Materials Science beamline P21.2 at the synchrotron PETRA III at DESY, Hamburg, Germany. The photon energy used was 96 keV (0.1291 Å) and the distance between the sample and the Varex 4343CT flat panel detector was about 1.6 m. LaB6 was used for geometry calibration. The sample surface was aligned to be parallel to the X-ray beam which was 20  $\mu\text{m}$  (vertical) x 55  $\mu\text{m}$  (horizontal) large. The entire specimen was scanned in 20  $\mu\text{m}$  steps across the entire specimen thickness. The 2D diffraction images were converted into 1D patterns using integrating the diffraction data along all azimuthal angles using pyFAI. The HEXRD signals were measured in transmission mode while the sample was scanned from the surface down to the bulk, so the diffraction data provide the information of the lattice deformation (strain development) in the microstructure of the entire sample, which can be viewed as a function of depth, i.e., in-depth profile. We plan to perform the same HEXRD measurement of the 9 months samples in 2021.

### **3.3.8 Scanning Kelvin probe force microscopy (SKPFM)**

SKPFM was employed to measure the Volta potential difference (VPD) between tip (platinum) and the surface of the specimens with different exposure conditions. The Dimension Icon from Bruker with OSCM-Pt R3 probes from Olympus was used. The measurements were conducted in ambient air environment at 22°C and 23% relative humidity. The map resolution was 256 x 256 pixels. The nullifying bias was applied to the sample to show noble regions as high

potentials, implying cathodic character, and less noble regions as low potentials, implying anodic character, in the Volta potential maps.

### **3.3.9 Additional test for glass-sulphide interactions**

Additional experiment was conducted in 2020 to study the leaching of borosilicate glass. The results from the first experiments suggest that there might have been a reaction in test vessels between the borosilicate container material and the used solution. The reaction was observed as white distinct sediment was found in test vessels with 32 mg/L or more sulphide added. Also, the water analysis showed elevated values for boron and silicon.

In this additional test set, 320 mg/L and 640 mg/L water samples were prepared similarly than in all exposures. The chemical parameters of both of waters were analysed in similar manner as described in 3.3.4. In addition, copper sheets were placed in “normal laboratory” borosilicate glass vessel (“bottle A”) and borosilicate glass vessel from another manufacturer (“bottle B”) to study the difference in glass quality. Bottles which were filled with test solutions and kept for 42 days at room temperature. Afterwards, water samples were collected and analyzed.

## 4. Results and discussion

### 4.1 Corrosion measurements

#### 4.1.1 Electrochemical measurements (Test initiated in 2019)

The electrochemical measurements were conducted in designated bottles. The measurements across the duration of the test enabled seeing the trends in corrosion rates throughout the test. For measurements started in 2019, most of the results, including Tafel and LPR, are reported in the first annual report (Ratia et al., 2020). EIS results were analyzed in 2020 and are presented in the following.

In general, the impedance spectra for copper samples in the groundwater environment change considerably with time of exposure, and the comparison between the exposures without and with sulphide show clearly the effect of sulfide on the corrosion process. Depending on the sulphide level of the exposure environment (0, 32 mg/L or 320 mg/L) and the time of exposure (0 to 181 days), the EIS spectra from the samples showed either one, two, or three time-constant features. In each exposure environment, the behaviour changed during the test, so the EIS data are treated in two parts in each case.

In the environment without sulphide, the spectra for the first 22 days showed two time-constants features, Figure 1, which may be attributed to the response from an inner compact layer and porous outer layer of the corrosion products, most likely oxides and hydroxides of copper with incorporation of ions from the ground water. The two time-constants are not well separated in frequency (or time) domain, so it is difficult to obtain accurate data from the spectra fitting. After 32 days, the spectra in Figure 2, showed three time-constants ( $\tau_1$ ,  $\tau_2$  and  $\tau_3$ , marked in the Bode plot of phase angle), where the third constant could be attributed to diffusion of some reactive species in the porous layer. The change in the EIS feature from two time constants to three time constants is likely due to the change of the structure of the corrosion product film, e.g., “sealing” of the porous outer layer due to precipitated compounds inside the pores, as observed on anodized aluminum. As a result, the impedance modulus at low frequencies (a measure of polarization resistance) increased with exposure time, see Figure 1 and 2, Bode plots of impedance modulus.

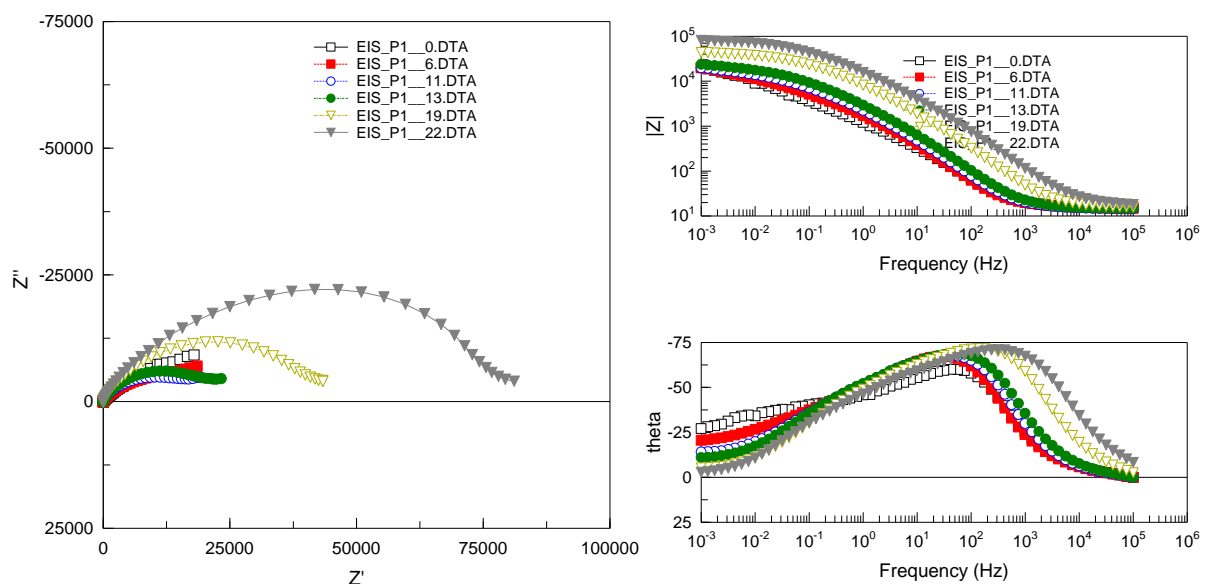


**Figure 1.** Impedance spectra for sample exposed to simulated groundwater with no sulphide addition. Nyquist plot (left) and Bode plots (right) from day 1 to day 22.

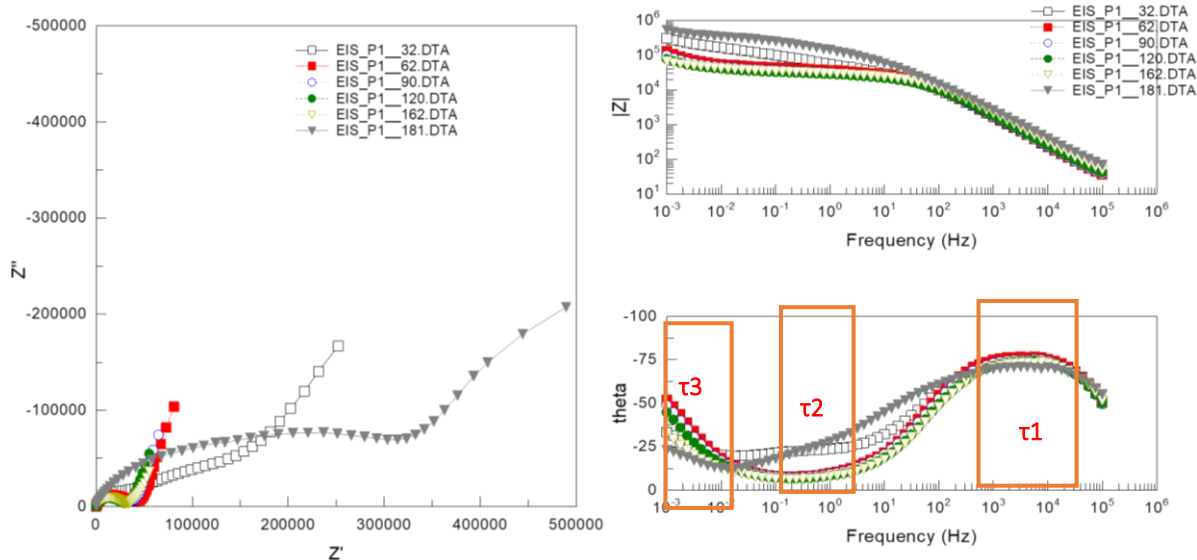


**Figure 2.** Impedance spectra for sample exposed to simulated groundwater with no sulphide addition. Nyquist plot (left) and Bode plots (right) from day 32 to day 181.

In the case of exposure with 32 mg/L sulphide, the EIS spectra remained quite similar, showing two time-constants for the first 120 days as shown in Figure 3. Afterwards, the spectra exhibited three time-constants features (Figure 4). The model for a layered structure, i.e., an inner compact layer and porous outer layer, of the corrosion products mentioned above, also can be used for interpretation of these EIS spectra. The two-layer corrosion products give rise to the two time-constant responses at high and middle frequency ranges, and the diffusion process gives rise to the third time constant at lowest frequencies. It should be noted that, the impedance modulus at low frequencies is generally lower than that for the exposure without sulphide, and even decreased after prolonged exposure, see Figure 3 and 4, Bode plots of impedance modulus. This indicates that, in the presence of sulphide the corrosion product film is less protective, and may even become weaker with time.

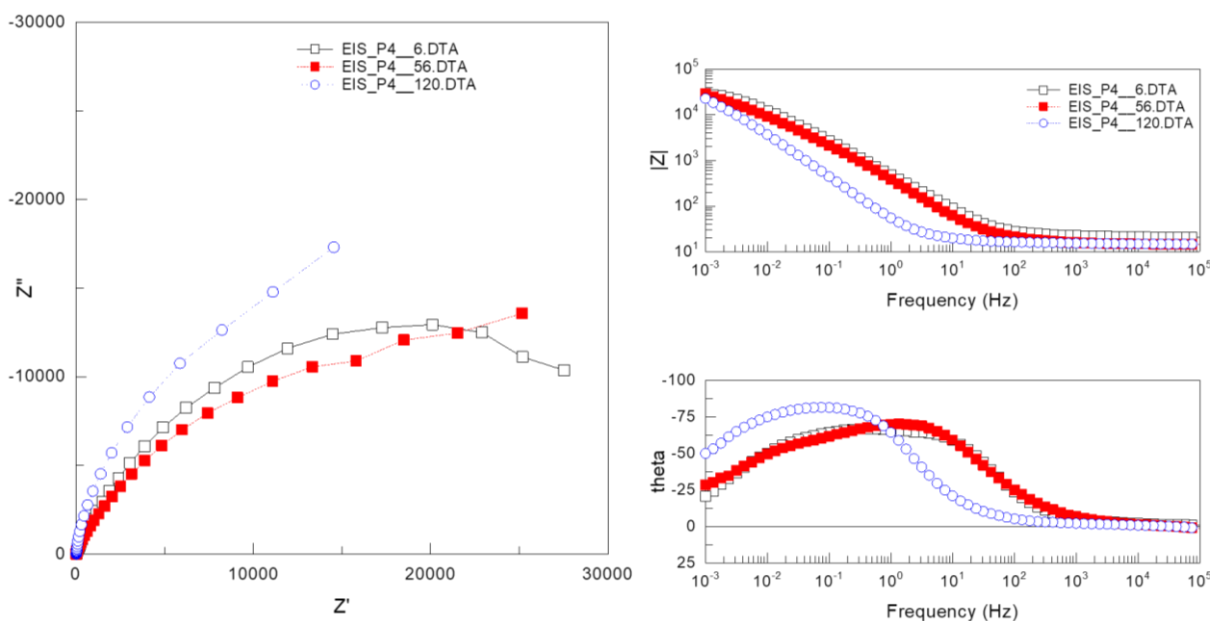


**Figure 3.** Impedance spectra for sample exposed to simulated groundwater with 32 mg/L sulphide addition. Nyquist plot (left) and Bode plots (right) from day 1 to day 120.

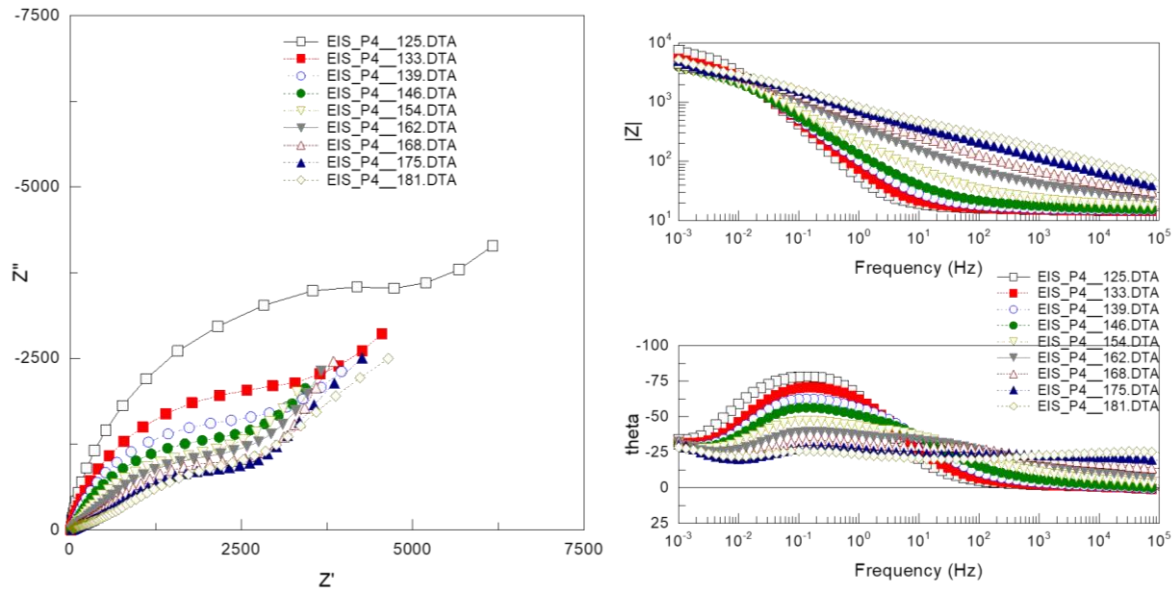


**Figure 4.** Impedance spectra for sample exposed to simulated groundwater with 32 mg/L sulphide addition. Nyquist plot (left) and Bode plots (right) from day 125 to day 181.

In the environment with the highest sulphide content, 320 mg/L, the EIS spectra showed essentially one time constant from the beginning to day 22 (Figure 5), and two time-constants from day 32 and afterwards (Figure 6). This indicates that the corrosion process and the development of the corrosion products on the copper surface are quite different from the environments without sulphide or with a low level of sulphide content. In the early stage, probably no protective corrosion product film is formed, so the copper-electrolyte interface gives rise to one time constant feature of the EIS, whereas in the later stage, a corrosion product film is formed giving the two time constants of the EIS features, but the film is not protective against corrosion, as judged from the low value of impedance modulus at low frequencies.

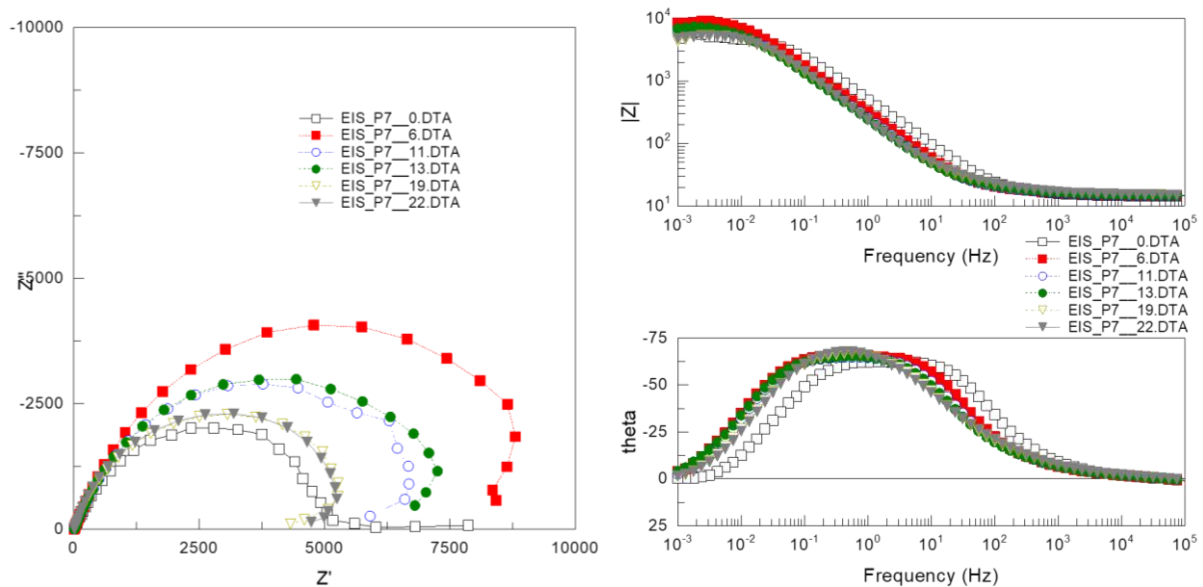


**Figure 5.** Impedance spectra for sample exposed to simulated groundwater with 320 mg/L sulphide addition. Nyquist plot (left) and Bode plots (right) from day 1 to day 22.

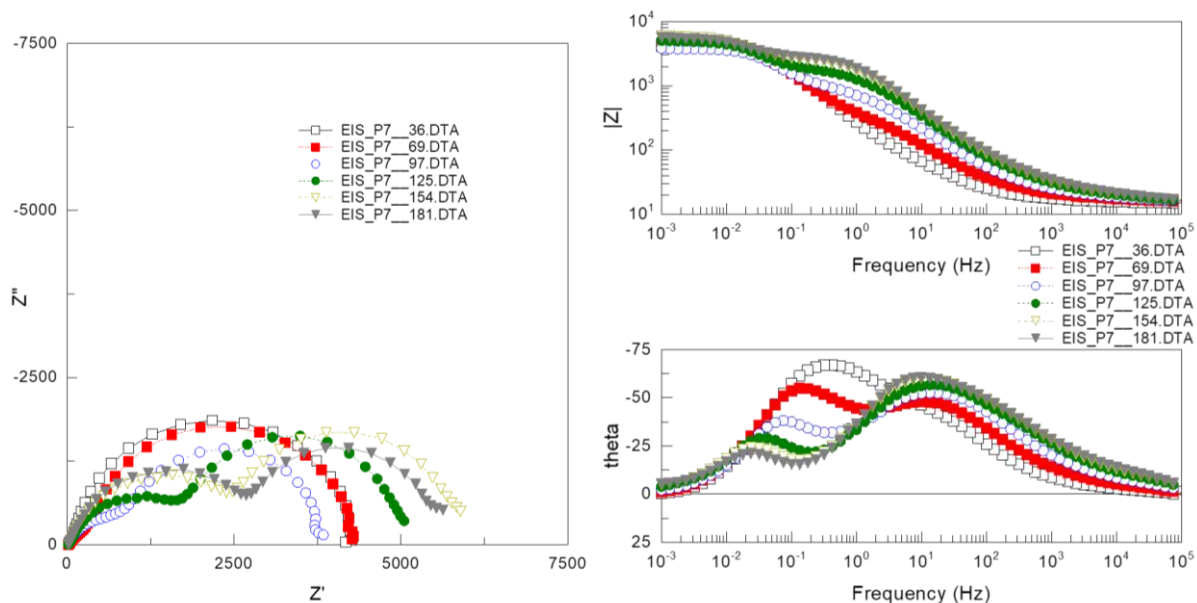


**Figure 6.** Impedance spectra for sample exposed to simulated groundwater with 320 mg/L sulphide addition. Nyquist plot (left) and Bode plots (right) from day 32 to day 181.

The EIS results also show that, with a high level of sulphide in the environment, the impedance modulus at low frequencies is more than one order of magnitude lower for the exposure with high content of sulphide than that for the exposure without sulphide. This indicates that the presence of sulphide, especially at a high level, enhances the corrosion rate of copper in the environment. Moreover, the lower corrosion resistance and thus higher corrosion rate remained until 181 days of exposure (termination of the measurement), implying that the corrosion process was not impeded by the formation of the corrosion products on the surface.

The EIS features could be described by equivalent circuits corresponding to an inner compact layer, a porous outer layer of the corrosion product film, and diffusion effect. The EIS data could be fitted by using the equivalent circuits shown in Figure 7, corresponding to one, two, and three time-constants, respectively.

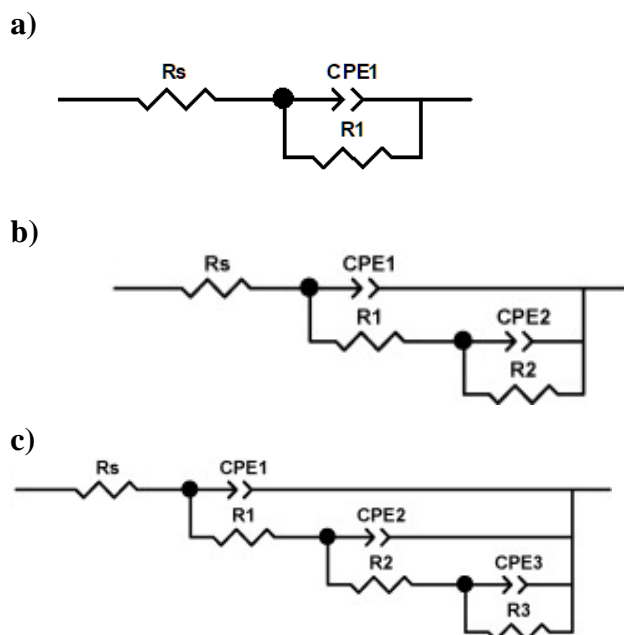


**Figure 7.** Equivalent circuits used in fitting the impedance data: a) one time constant circuit, b) two time constant circuit, c) three time constant circuit.  $R_s$  correspond to solution resistance (of electrolyte), CPE stands for constant phase element accounting for non-ideal capacitive response, and R for different resistances corresponding the polarization resistance, the resistance of the porous layer, and charge transfer resistance at the copper-electrolyte interface, respectively. Approximately, the low frequency modulus corresponds to the sum of these resistances.

In general, the EIS spectra measured for the copper samples exposed to the ground water containing different levels of sulphide and after different time intervals indicate the formation and change of the corrosion product film and its protection effect with the time of exposure, which is influenced by the level of the sulphide in the ground water. Because in some cases, the time constants are not well separated in frequency (or time) time domain, the use of the equivalent circuit may be somewhat ambiguous, and it is difficult to obtain accurate and meaningful values for the circuit elements, so the fitting data are not given here. Nevertheless, the semi-quantitative interpretation of the EIS results already provide useful information about the influence of sulphide in the corrosion process and the change with exposure time up to 181 days. Some experimental evidences about the corrosion products are very helpful to support the interpretation of the EIS results. Ideally, the analysis of the cross-section of the exposed samples should be done to exam the postulated layered-structure of the corrosion product film.

#### 4.1.2 Electrochemical measurements (8- and 9-month tests)

The first electrochemical test initiated in 2019 and had length of 8 months. New 9-month long test series, that was started in 2020 is still on going and all the results will be reported in the Final report 2022. The OCP and redox values were continuously monitored during both tests. The OCP and redox values in the first test initiated in 2019 are presented in Figure 8. Unfortunately, an oxygen leakage was detected as the solutions contained significant amount of oxygen after the test, and thus, these results are debatable. Therefore, a new, improved and partially parallel test was initiated in 2020.

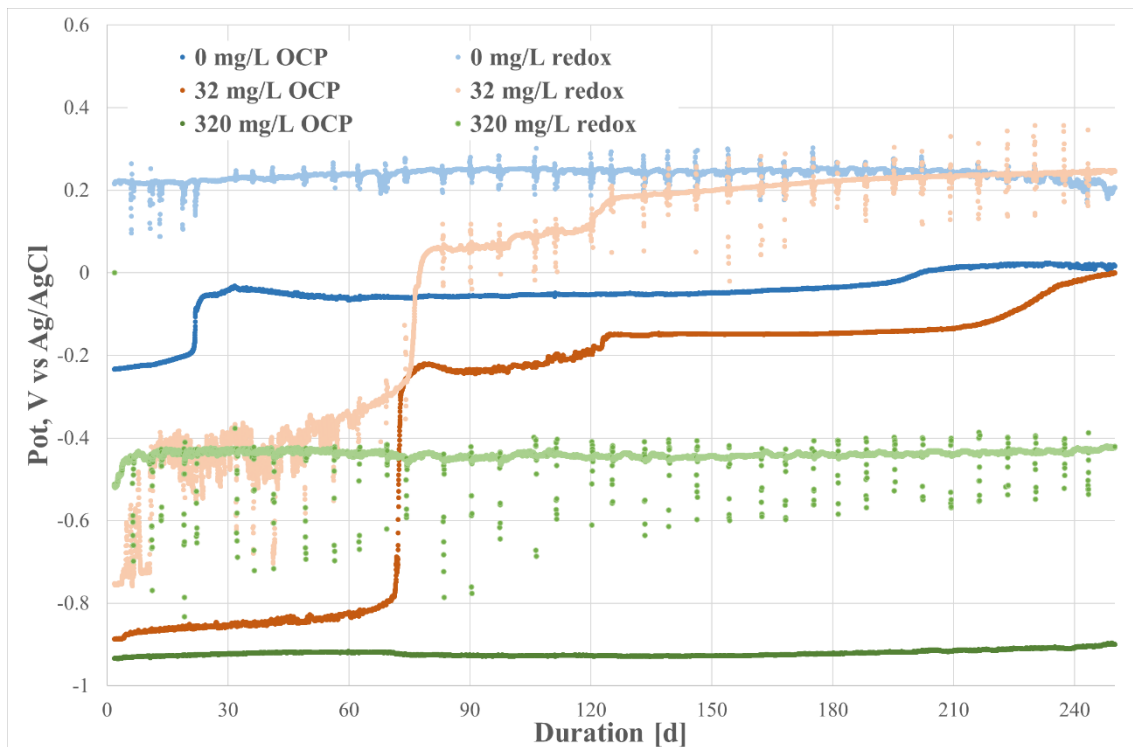


**Figure 8.** OCP and redox potential values for the 2019 initiated 8-month test.

In the on-going new test, Figure 9, (data showed for the first 223 days) the highest OCP and redox values were recorded in environment with lowest sulphide content (3.2 mg/L). In previous experiment conducted in 2019, a distinct increase in the OCP was detected after 70 days of 32 mg/L samples. It was speculated that the increase in OCP could be attributed to the fact that sulphide in the water had been consumed by chemical reactions. However, in this 9 month experiment similar increase in potential in 32 mg/L samples (red in Figure 9) was not observed. To further study this mechanism, increase of potential after sulphide is consumed, a vessel with intermitted  $\text{Na}_2\text{S}$  additions were used. The initial sulphate content was 3.2 mg/L and with intermitted additions of  $\text{Na}_2\text{S}$  the final concentration was targeted to be 320 mg/L. In this test vessel (green in Figure 9), similar distinct increase in potentials were seen first after 85 days. First  $\text{Na}_2\text{S}$  addition was done after 132 days and caused significant drop in potential reaching a lower potential than in the beginning of test. Another increase in potentials after 175 days were compensated again with  $\text{Na}_2\text{S}$  addition resulting in another significant drop to even lower potential values. This experiment is still on-going and one more  $\text{Na}_2\text{S}$  addition is planned. The LPR and Tafel results of this experiment will be presented in Final report of the project.

It seems that sudden increase in the OCP and redox potential is related to the oxidation or consumption of sulphide, since the zero sulphide had higher potential values and did not show such increase. In addition, the highest sulphide level (320 mg/l) had low potential values and did not show such increase (probably not consumed completely).

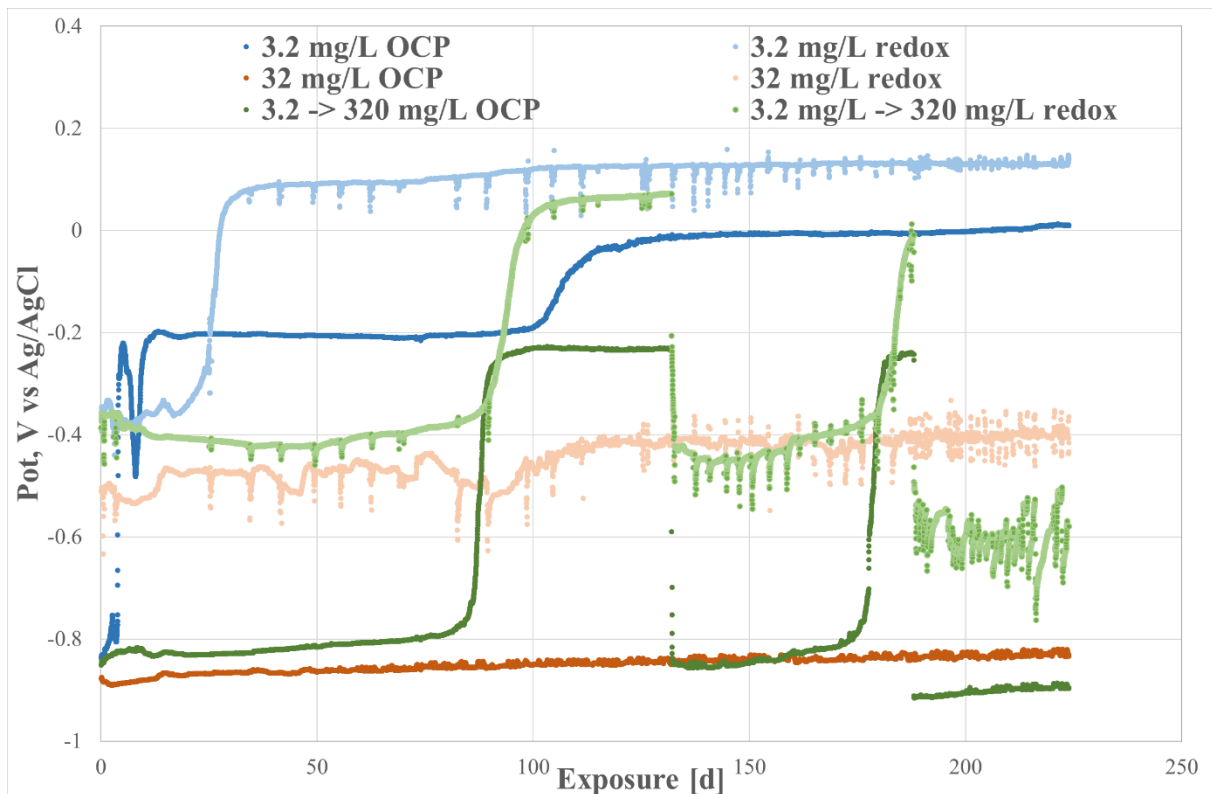


**Figure 9.** OCP and redox potential values for the first 223 days of currently on-going 9- month experiment.

The first long electrochemical measurement experiment showed interesting features in the OCP and redox monitored online. However, since possible oxygen leakage was detected in the measurements after the exposure, the test results are not unambiguous, and the oxygen may have a role in the chemical reactions causing the distinct changes in electrochemical behaviour. This is supported by the fact that also the simulated groundwater without sulphide additions (0 mg/L) had clear step in the OCP curve indicating that the steps cannot be explained exclusively by the point where all sulphide is reacted in the solution. However, in all other cases, the sudden increase in OCP is always been simultaneous with increase in redox. For this 0 mg/L case, the redox did not show such increase. In the new experiment, the observation was repeated – sudden increases in potential values of certain test vessels were seen. However, there is no consistent trend that certain sulphide content would lead to this behaviour. Polarization resistance and EIS-measurements performed simultaneously with these OCP measurements may provide addition information about the behaviour and changes before and after the potential increase. This data will be analyzed after the test ends in 2021. Also, the oxygen level of the solution can be measured only after termination of the test. This value will be important to evaluate the role of oxygen in the reactions. If oxygen leakages are avoided with the improved system used at the moment, more conclusions can be drawn on the role of sulphide films. Naturally also careful sample characterisation after the test will be made in 2021 to support and explain the findings.

#### **4.1.3. Corrosion rate and mass loss (4-month experiment)**

Results from 4-month experiment initiated in 2019 are presented here. All mass loss results are converted into corrosion rates ( $\mu\text{m/a}$ ). The corrosion rates of the pre-oxidised samples were slightly higher than samples without pre-oxidation in all three environments, as seen in Table 3 and Figure 10. However, there was deviation in results and the differences due pre-oxidation are within the limits of deviation, Figure 10. The finding that pre-oxidised samples suffer higher

mass losses was encountered before by the authors in copper exposed in simulated groundwater at 37 °C (Isotahdon et al., 2019).

**Table 3. Average corrosion rates.**

S content	Sample	Average corrosion rate, $\mu\text{m/a}$
0 mg	ground	0.258
	pre-oxidized	0.320
32 mg	ground	0.384
	pre-oxidized	0.396
320 mg	ground	0.325
	pre-oxidized	0.329

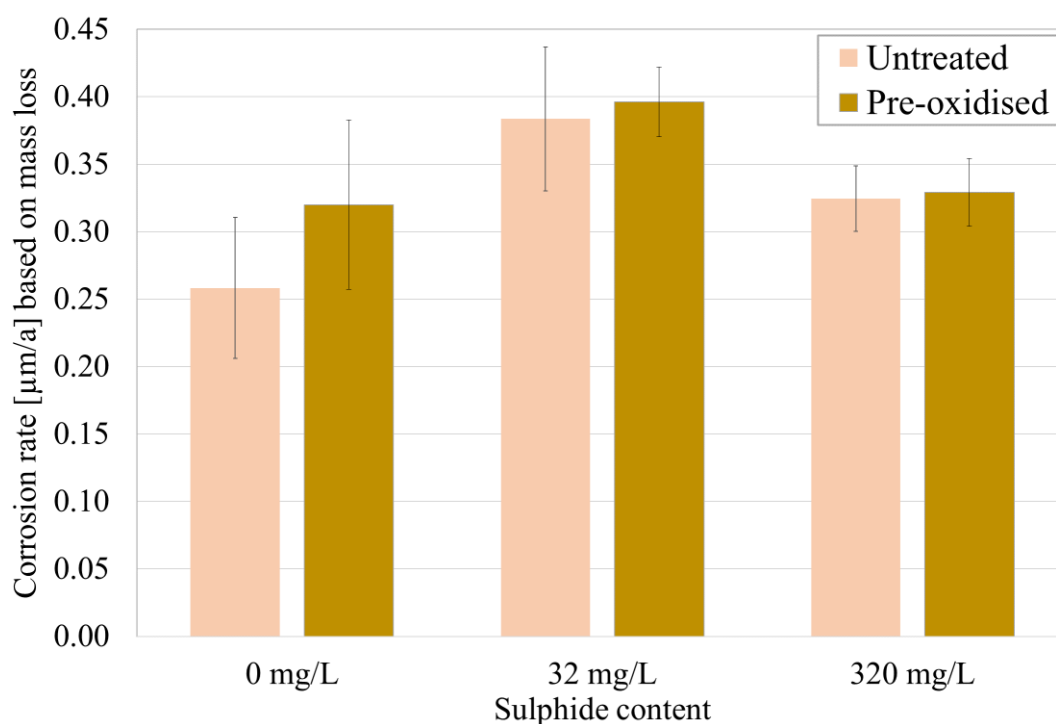


**Figure 10.** Average corrosion rate based on the mass losses of ground (untreated) and pre-oxidised OFP-copper samples with varied sulphide content in the simulated groundwater during 135 day of exposure. The error bars represent standard deviation.

One of the most interesting findings was that the highest corrosion rates were obtained for samples exposed to sulphide content of 32 mg/L. The mechanisms are not unambiguous, but the addition of sulphides in the simulated groundwater indeed increased the mass losses of the samples compared to that without sulphide. Literature includes studies with corrosion resistance decreasing when sulphide concentration is increased (Kong et al., 2017). However, the sulphide concentration is related to nature of the  $\text{Cu}_2\text{S}$  layer (Chen et al., 2011) and protectiveness is affected also by other components present. The protectiveness and nature, in terms of e.g. pores present of the ability to passivate, of the sulphide film will most likely attribute the weight losses.

The visual observations of these samples were already reported in the annual report 2019. To summarize the observations, test environments with 32 mg/L and 320 mg/L had flaky white sediment on the test bottle. Also, it was noticed that in some samples, especially with the 32

mg/L samples, Na<sub>2</sub>S granules had not fully dissolved in solution and thus they had landed on the sample surface causing burnt marks. These local defects most likely attribute also to the highest mass losses recorded. SEM observations reported earlier in first annual report (Ratia et al., 2020) support the fact that a lot of local differences can be found between each sample surface. These findings give complexity to analysis of surface films.

When compared to the corrosion rates obtained with electrochemical methods and reported earlier (Ratia et al., 2020), the mass loss -based corrosion rates seem to be considerably lower. The momentary corrosion rates obtained and calculated with the  $I_{\text{corr}}$  determined by extrapolating from Tafel plots were between 0 and 12  $\mu\text{m/a}$  depending on the sample and measurement time. Corrosion rates calculated based on LPR measurements were between 0 and 8  $\mu\text{m/a}$ . The corrosion rate of the 320 mg/L sulphide content were highest during most of the measurement period, according to both electrochemical methods used (EIS and LPR). Although some momentary high peaks in corrosion rate were also detected for 32 mg/L samples with electrochemical methods.

#### **4.2 More detailed surface characterisation of samples from experiments initiated in 2019**

Sample characterisation of the first 4-month experiment samples was started in 2019 and mostly reported in annual report 2019. The work continued in year 2020. In addition to visual characterisation and SEM+EDS results reported in previous report, GIXRD and Raman characterisation was performed. Also, the samples used for the first electrochemical measurements were characterised using SEM.

##### **4.2.1 SEM EDS study of the surfaces of electrochemical samples**

The electrochemical measurement system consisted of three parallel samples, A, B and C, in each environment (0 mg/L, 32 mg/L and 320 mg/L of sulphide). A-samples were used for linear polarization and EIS measurements, B-sample for open circuit potential measurements and C as reference when needed. That means that sample A was polarised and possible surface films may have been destroyed in the process, whereas B and C were exposed to more stable conditions. All sample surfaces from the first 8-month experiment were studied with SEM and EDS in 2020. SEM SE images of electrochemical (EC) samples used in 0 mg/L, 32 mg/L and 320 mg/L tests are presented together with photograph of each sample after the exposure in Figures 11, 12 and 13, respectively.

Samples exposed to simulated groundwater (0 mg/L S<sup>2-</sup>) had quite even corrosion product layer on the surface. The visual observations are that the colour of samples have changed more from original bright copper to darker brownish (Figure 11). The topography in SEM images could refer to copper oxide. When compared to visual observations after the 4-month immersion test in 2019, longer test evidently changes the surface colour more. It must be noted that these EC samples are not pre-oxidized. According to EDS analysis the surface layer that is most likely precipitation layer comprised of about 40 atomic-% (later at%) O whereas the amount in the areas of pits or cavities were less. In sample C SEM-image of the pit bottom number 1 in Figure 11 had only 5 at% of O, whereas the surrounding corrosion layer marked as 2, had 55 at% of O, small amounts of Al, Si and Cl as impurities and rest of Cu. This indicates that the corrosion product layer, and thus the corrosion attack, is not uniform on the copper surface, even without addition of sulphide in the ground water, probably due to the heterogeneous microstructure of the copper sample, leading to a non-uniform formation/deposition of the corrosion products on the surface.

SEM SE, 0 mg/L electrochemical samples

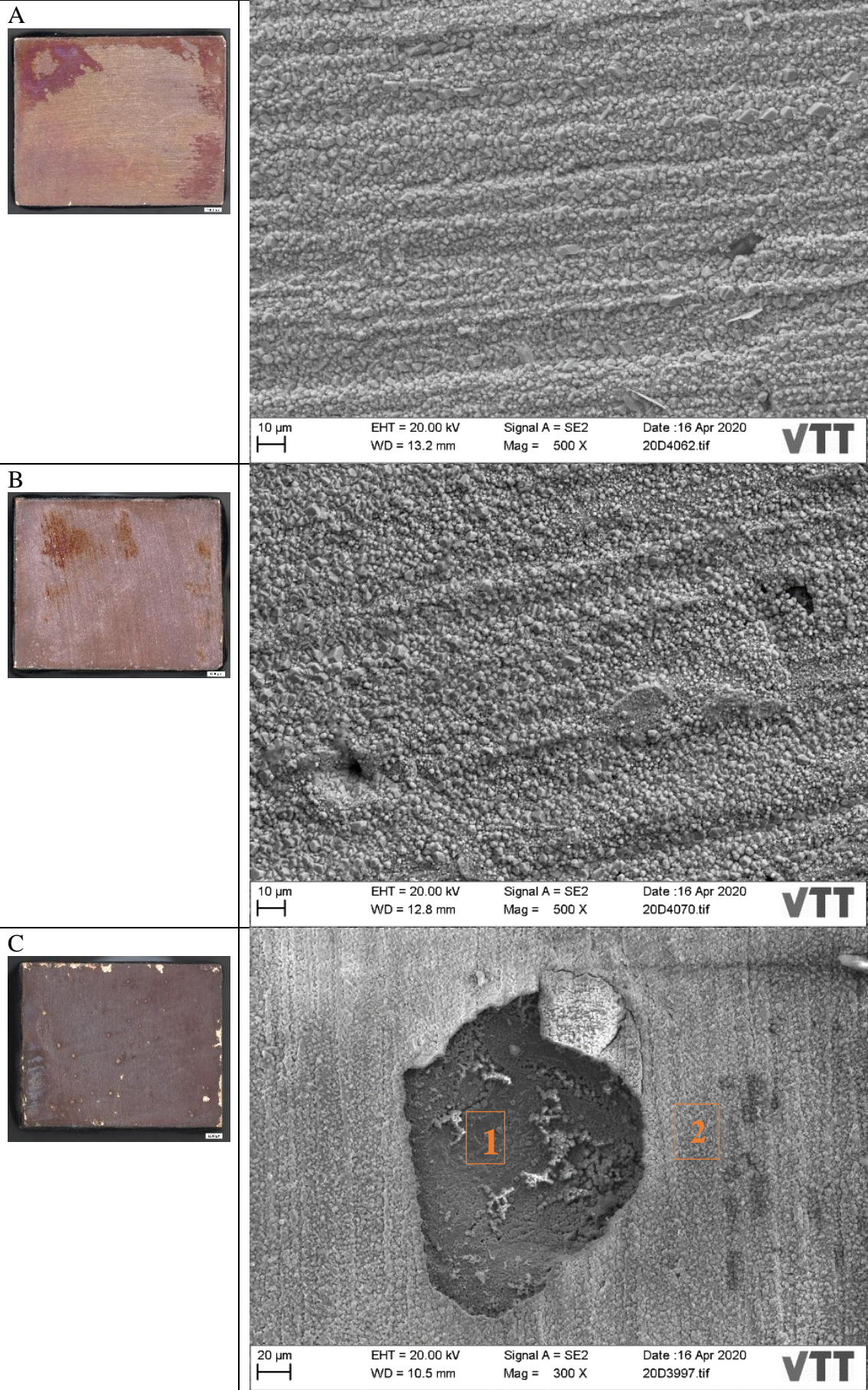


Figure 11. SEM SE images of electrochemical samples A, B and C in 0 mg/L  $\text{S}^{2-}$  environment.

The corrosion product or precipitated layers on the surfaces of EC samples in 32 mg/L  $S^{2-}$  environment (Figure 12) were darker in colour and visually differed from each other. The surface product layer appeared more detached, as bright copper could be detected where the layer has dried and cracked. Cracking has occurred after taking sample out from the test, as the surface layer has dried. Overall, the EDS showed very similar oxygen content as in the 0 mg/L samples. Around 50 at% O was found. The amount of sulphur that EDS could detect was mainly only 0-2 at%. However, the fluffy corrosion product in C sample marked with number 1 and arrow in Figure 12, had a composition of 50 at% O, 4 at% S, 10 at% Cl and 32 at% Cu. Highest sulphur content sites were detected along highest chloride content. The corrosion product layer is not uniform and there are sulphur-rich sites.

The corrosion product layers on the surfaces of EC samples in 320 mg/L  $S^{2-}$  environment (Figure 13) are almost black in colour. In A and B samples, the surface layer has cracked due to drying of thick deposit layer and peeled off as seen in photograph. Very different local surface details were found in SEM imaging, depending on the site of imaging. In most parts of sample surface, EDS did not show any traces of oxygen containing deposits of layers. The overall S contents were significantly higher, as expected. In most locations about 30 at% of S was found in all three (A, B and C) samples exposed to this environment. Very small amounts, <0.5 at%, of Ca ja Cl were found in surface layer.

SEM SE, 32 mg/L electrochemical samples

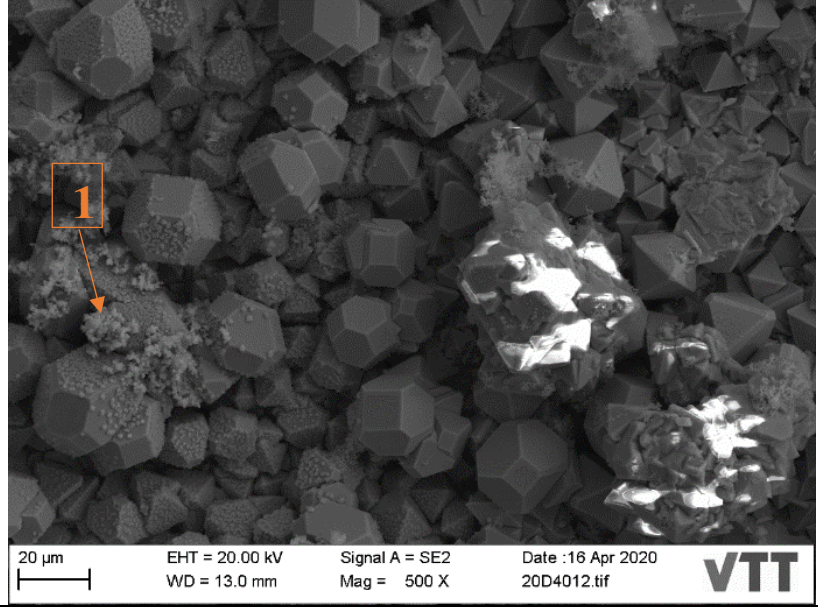
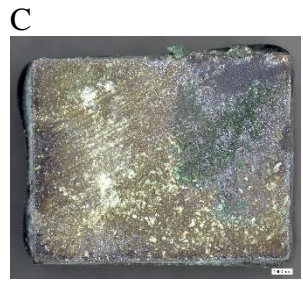
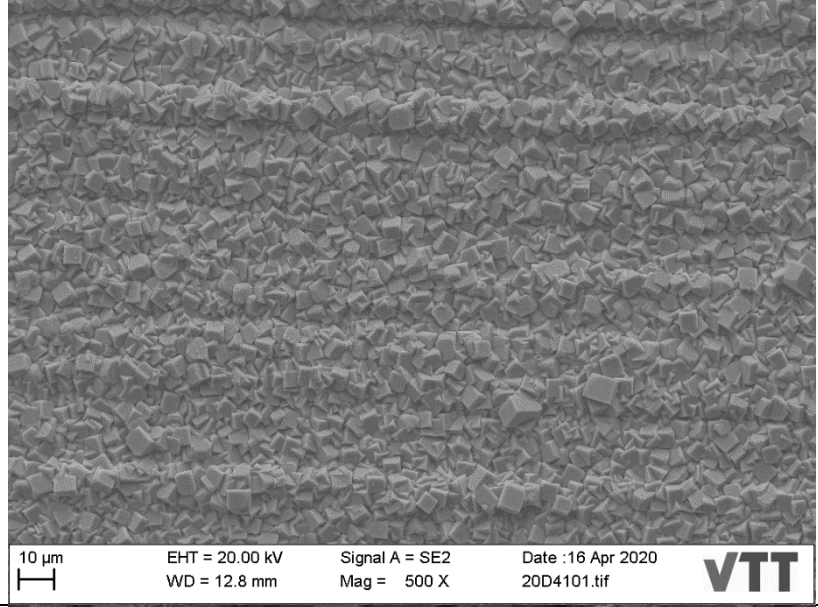
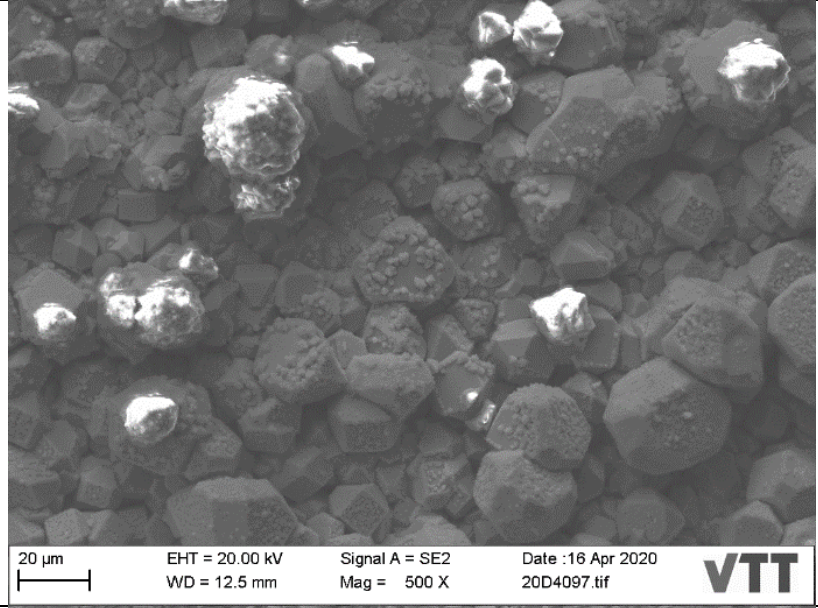
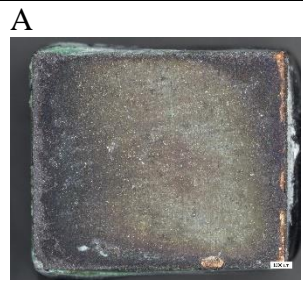


Figure 12. SEM SE images of electrochemical samples A, B and C in 32 mg/L S<sup>2-</sup> environment.

SEM SE, 320 mg/L electrochemical samples

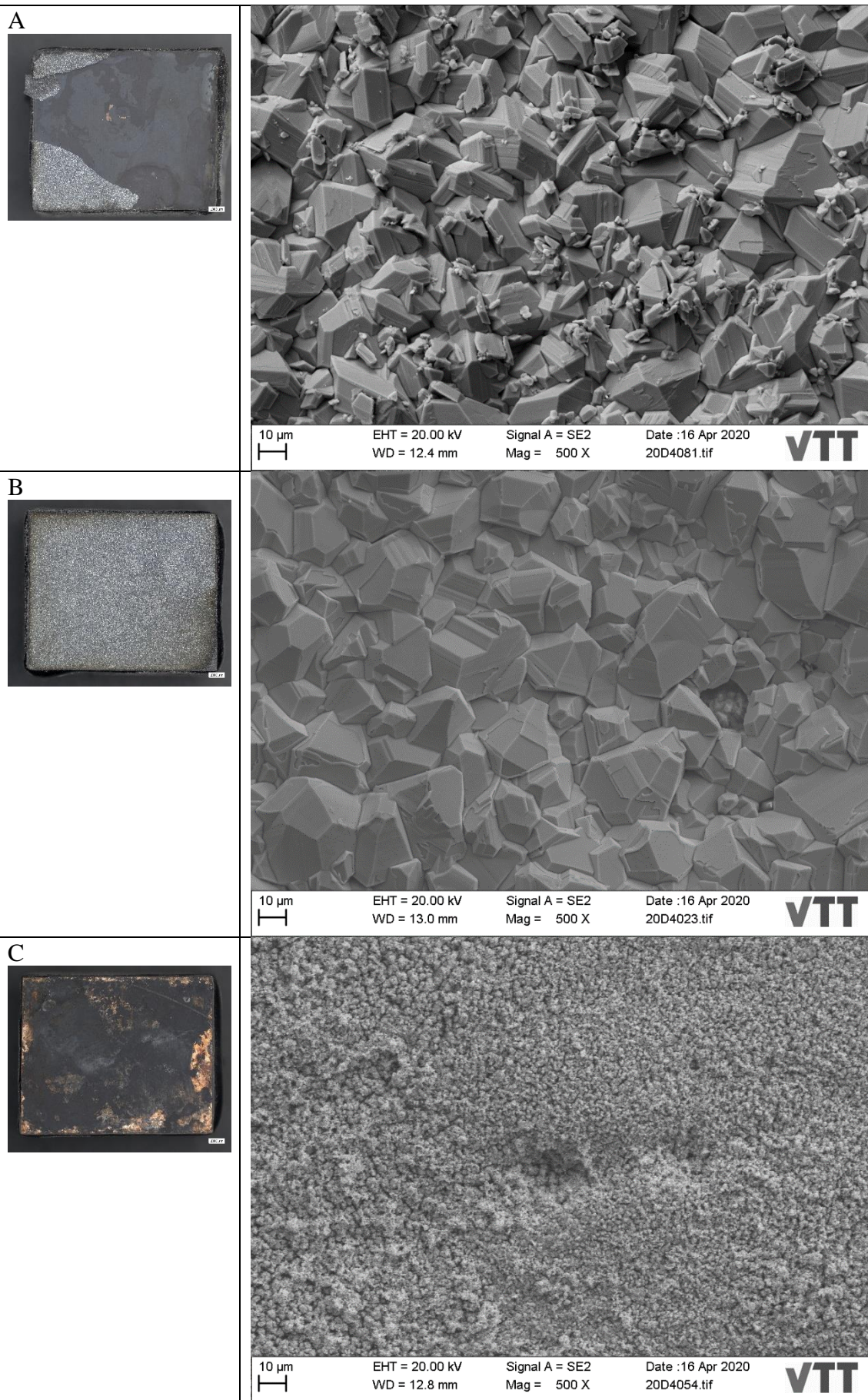


Figure 13. SEM SE images of electrochemical samples A, B and C in 320 mg/L S<sup>2-</sup> environment.

SEM study of the samples used in first set on electrochemical measurements gave us information on the surface condition after longer immersion period. Although EC-samples are not pre-oxidized, the amount of oxygen in surface films characterised with EDS was significant in the samples from 0 mg/L and 32 mg/L sulphide environments. The amount of oxygen could be linked to potential oxygen leakage and observations on unstable OCP behaviour in Figure 8. The presence of sulphur in the surface layer was not homogenous in 32 mg/L sample. In sample exposed to 320 mg/L sulphide, the sulphur content of surface layer was relatively constant, around 30 at.%, indicating precipitation of sulphur-containing surface layers. In future SEM and EDS studies, cross-sectional samples will be used to reveal better the possible surface structure.

#### **4.2.2 GIXRD and Raman studies**

The aim of GIXRD study was to analyze the thin corrosion product and other surface layers present in the sample surface. Previously, traditional XRD analysis was conducted, but the resolution was not enough to detect the thin surface layers. GIXRD patterns of the surfaces of samples that were in initial state (not exposed) and those that were exposed to various sulphide concentrations are presented here.

Naturally, the presence of pure Cu was found in unexposed samples (Figure 14). Also, the presence of CuO was detected in samples exposed to natural groundwater (Figure 14 b). The surface state (pre-oxidized, not pre-oxidized) affected the XRD data so that peak broadening and splitting was observed. Based on the intensities, the corrosion product layers on pre-oxidized samples were thinner than untreated samples. In addition to CuO, only CuS could be detected in the case of pre-oxidized sample exposed to 320 mg/L environment (Figure 15). Indicating that pre-oxidizing step in controlled temperature and humidity results in thin, evenly distributed oxide film that protect the sample from sulphide attack except in the highest sulphide concentrations. It is also likely, that the corrosion layers are too thin to be detected by means of XRD, and some compounds are overlooked. However, the lower intensity of Cu peaks in certain cases indicates the possibility of an amorphous layer formed on the surface. This finding will be further studied.

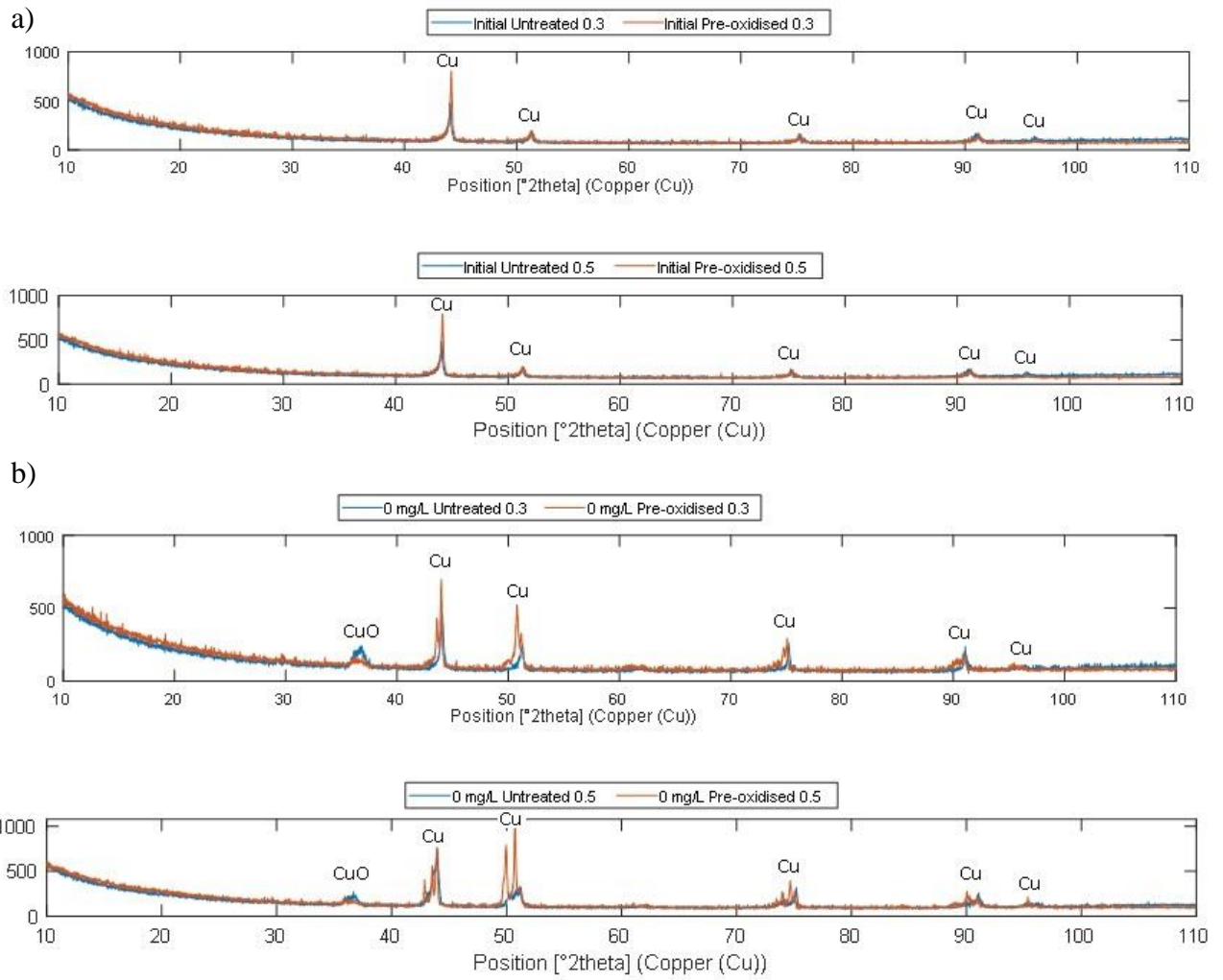


**Figure 14.** Grazing incidence angle XRD patterns of the surfaces of the polished characterisation samples in untreated and pre-oxidised states: a) initial (not exposed), and b) exposed to simulated groundwater (0 mg/L sulphide). The 0.3 and 0.5 correspond to the grazing incidence angle.

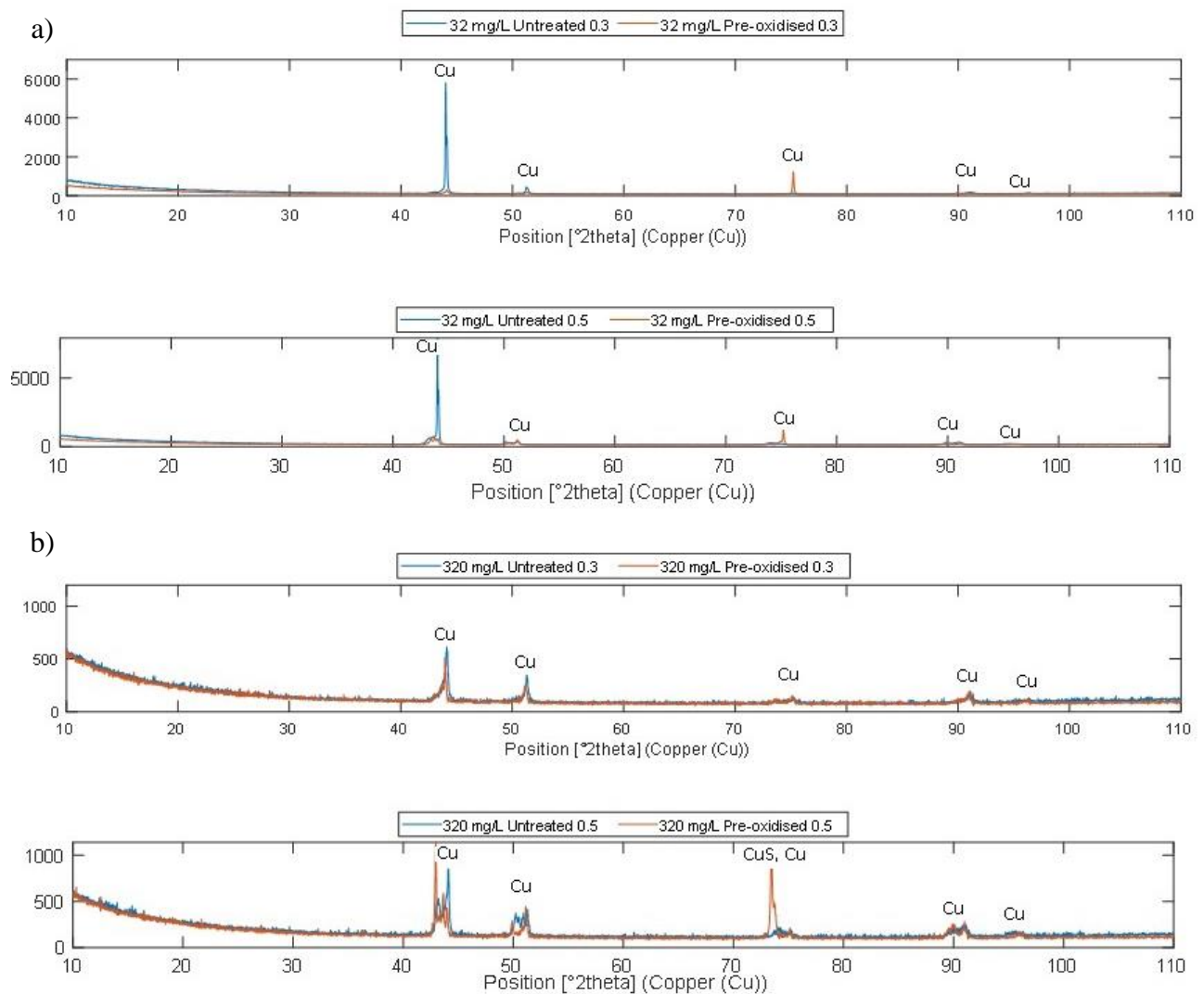


**Figure 15.** Grazing incidence angle XRD patterns of the surfaces of polished characterisation samples in untreated and pre-oxidised states: a) sulphide addition of 32 mg/L and b) sulphide addition of 320 mg/L. The 0.3 and 0.5 correspond to the grazing incidence angle.

The GIXRD measurements of the specimens exposed to the  $S^{2-}$  solutions resulted in reflexes for metallic copper and only a few weak signals originating from copper sulfide or oxide. This indicates that standard x-ray instrumentation is not sensitive enough for the examination of the thin corrosion product films formed during 4-month exposure.

Unfortunately, also Raman spectroscopic examinations didn't produce peaks that could be clearly related to corrosion products which can be expected to form on copper after an exposure to  $S^{2-}$  containing groundwater. In conclusion, both methods tested are not sensitive enough for samples used. However, it is possible that longer exposure time would result in thicker surface films that could be detected also by these means. Individual samples from 9-month exposure could be analysed using these methods to re-evaluated the suitability of analysis methods. For Raman studies, surface-enhanced Raman spectroscopy (SERS) should be used in future studies.

### Synchrotron GIXRD results

The synchrotron GIXRD provide more information of the corrosion products. The Cu peak profiles are not always homogeneous and the intensity varies greatly between the different reflections and samples in a non-systematic way. This could be due to the large grains in the

copper sample while the X-ray beam was relatively small, which makes it difficult to determine the strain precisely. Regarding the corrosion products, there are a lot of peaks in the diffraction pattern and many possible compounds since mixed oxides, sulphides and sulphates may be present. For simplicity, the crystalline phases of the corrosion products were determined by comparing to theoretical patterns generated with VESTA (Visualization for Electronic and Structural Analysis 3D visualization program) and the crystallography open database. The diffractograms are shown in Figure 16. The results show that, after the exposure to the ground water containing NaS<sub>2</sub>, the initial CuO peak almost disappeared. For the exposure with 320 mg/l NaS<sub>2</sub>, the major corrosion products can be detected are CuS, Cu<sub>2</sub>S, and CuS<sub>2</sub>. After the exposure with 640 mg/l NaS<sub>2</sub>, the intensity of the CuS, Cu<sub>2</sub>S, and CuS<sub>2</sub> peaks increased greatly, whereas CuO still might be present (a small peak). Moreover, the data of the copper lattice indicate the development of the strain in the surface layer, which is influenced by the sulphide content in the ground water. For example, a large relative lattice expansion ( $>10^{-3}$ ) was measured for the sample after the exposure with 640 mg/l NaS<sub>2</sub>.

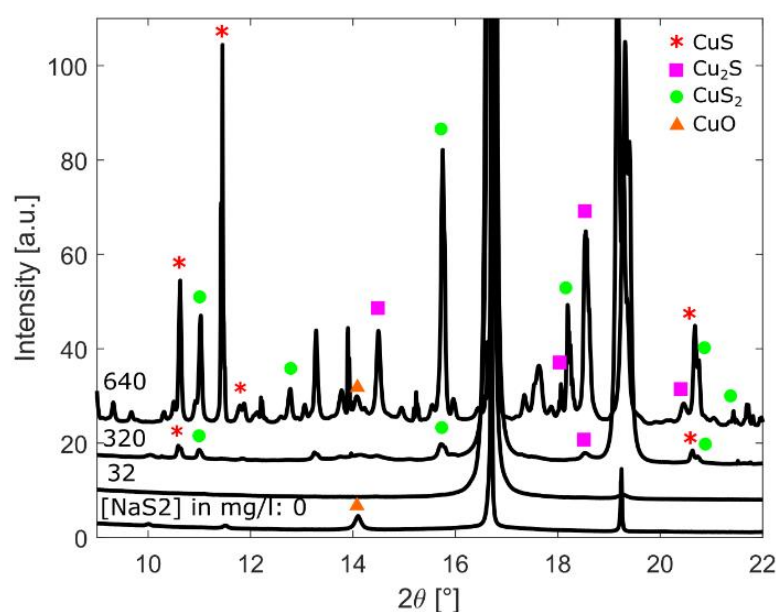


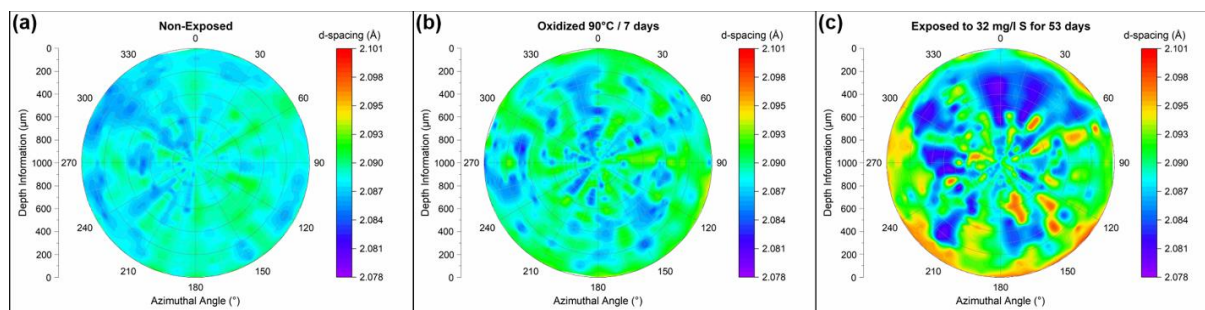
**Figure 16.** Diffractograms of the copper samples obtained from the synchrotron GIXRD measurements.

#### 4.2.3. Synchrotron HEXRD results and DFT calculation

The synchrotron HEXRD measurements of three 2-months samples yielded interesting results, showing clearly an effect of hydrogen infusion into the copper lattice, causing lattice degradation from the surface extending to ca. 90  $\mu\text{m}$  in the bulk. In combination with *ab-initio* density functional theory (DFT) calculation of the dissociation and adsorption of sulphur-species on copper surface and insertion of hydrogen in the copper lattice, the study has achieved a fundamental understanding of the role of sulphur and hydrogen in the corrosion of copper, which indicate a risk for hydrogen embrittlement of copper during exposure in the simulated ground water containing sulphide. These new findings have been published as an open access article at Corrosion Science, a high-ranking, peer-reviewed scientific journal in the research field.

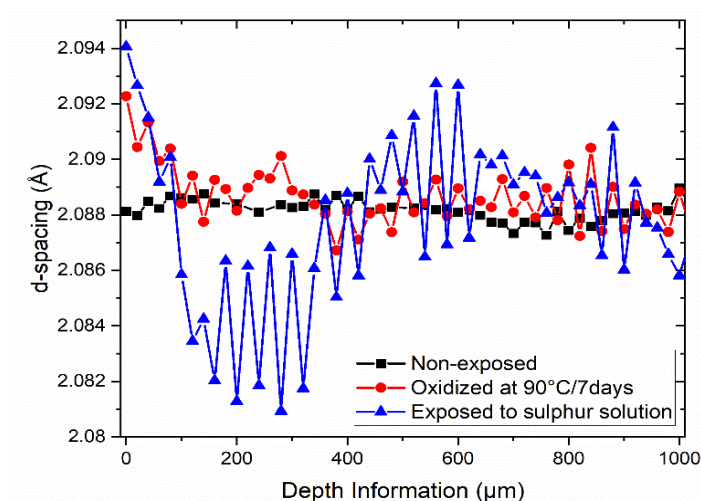
The key results are included here, in Figures 17-20, while the full article (Corrosion Science, 184 (2021) 109390) can be found at the link <https://doi.org/10.1016/j.corosci.2021.109390>. The d-spacing of the Cu lattice was determined. In Figure 17, the polar d-spacing plots of a non-exposed sample (reference), a pre-oxidized sample (oxidized), and pre-oxidized and exposed

to groundwater with 32 mg/L of sulfide. The polar plots show the calculated d-spacing as a function of the azimuthal angle and depth from the surface of the sample. The vertical axis on the left of each polar plot indicates the position inside the sample, with units in microns. The results show heterogeneous distribution of hydrogen-induced lattice deformation leading to significant high levels of local tensile strain (warm colour) in the microstructure.



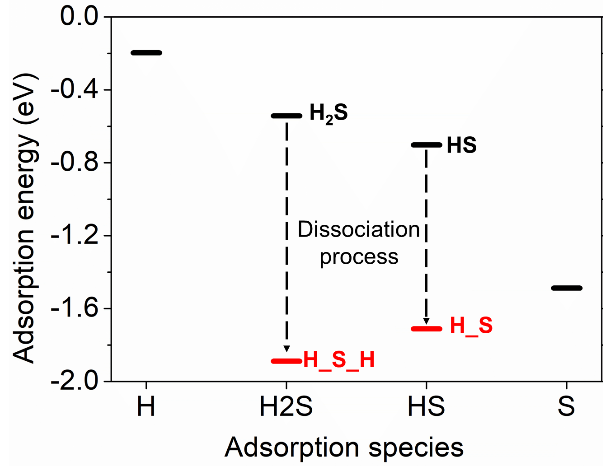
**Figure 17.** Polar plots showing the calculated d-spacing of the Bragg peak with (111) orientation as a function of depth from the surface and azimuthal angle for the copper specimens of (a) the non-exposed condition, (b) pre-oxidized at 90 °C for seven days, and (c) pre-oxidized and exposed to 32 mg/l of sulfide-containing groundwater.

Figure 18 shows the measured d-spacings plotted against the depth from the copper surface. The results show a significant hydrogen-induced expansion of the copper lattice (larger d-spacing than the non-exposed sample), and the relative lattice expansion reached a level of  $10^{-3}$  in the surface layer. DFT calculation of adsorption energies of  $H_2S$ ,  $HS$ ,  $S$  and  $H$  on  $Cu(110)$  surface was performed. The calculated adsorption energies are shown in Figure 19. The results show energetically favourable dissociation of  $H_2S$  and  $HS$  on the copper surface.



**Figure 18.** The measured d-spacings (integrated over the entire (111)-oriented 2D-diffraction ring) plotted against the depth from the surface of the copper specimens.

The configuration with one  $H$  atom and six surrounding  $Cu$  atoms are shown in Figure 20a, with calculated lattice relaxation by  $H$  insertion along different directions (Figure 20b-d). These results show hydrogen-induced lattice dilation (expansion) in  $Z$  (vertical) direction.



**Figure 19.** Calculated adsorption energies ( $E_{ad}$ ) of  $H_2S$  and  $HS$  in their molecular form ( $H_2S$ , or  $HS$ ), and full dissociation form ( $H\_S\_H$ , or  $H\_S$ ), and of individual  $S$  and individual  $H$ .

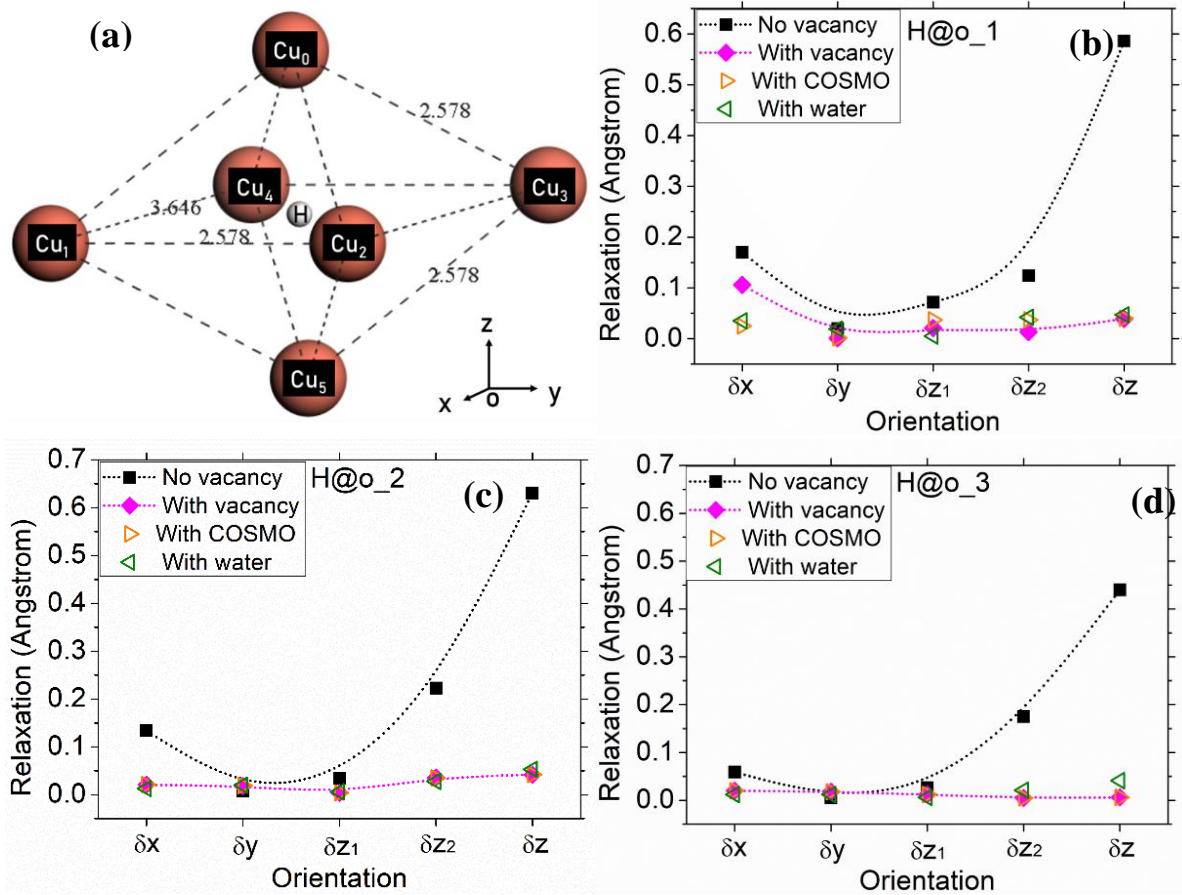


**Figure 20.** (a) Configuration (before optimization) with one  $H$  atom located at the center of the octahedron comprised by six  $Cu$  atoms, which gives initial atomic distances between two  $Cu$  atoms:  $Cu_{1-4} = Cu_{2-3} = 3.646 \text{ \AA}$  ( $x$  direction),  $Cu_{1-2} = Cu_{3-4} = 2.578 \text{ \AA}$  ( $y$  direction), while  $Cu_0$  and  $Cu_5$  are both  $2.578 \text{ \AA}$  away from the other four  $Cu$  atoms (denoted as  $z_2$ ,  $z_1$  direction, respectively);  $Cu_{0-5} = 2.578 \text{ \AA}$  are denoted as  $z$  direction. (b)~(d) Comparison between the relaxations induced by  $H$  insertion within  $o_1$ ,  $o_2$ ,  $o_3$  under differed situations.

#### 4.2.4. SKPFM results

The Volta potentials are given with respect to platinum ( $Pt$ ). The difference between features in a single map show the relative nobility, with lower values as less noble and higher ones as

more noble. Photograph of the scanned area, Topograph and Volta potential maps of the non-exposed sample are given in Figure 21, showing small variations in the height and Volta potential related to the Cu grains. Corresponding images for pre-oxidized sample in Figure 22 show large variations in the height and Volta potential, which are related to the differences in the oxide films on different grains of copper. Third studied sample was copper specimen exposed to 32 mg/L sulphide environment, and the AFM images in Figure 23 show even larger variations in the height and Volta potential than the un-exposed samples. The zoomed views show the heterogenous nature of corrosion product layer. Based on these images, precipitated surface layer consists of nodular-type particles.

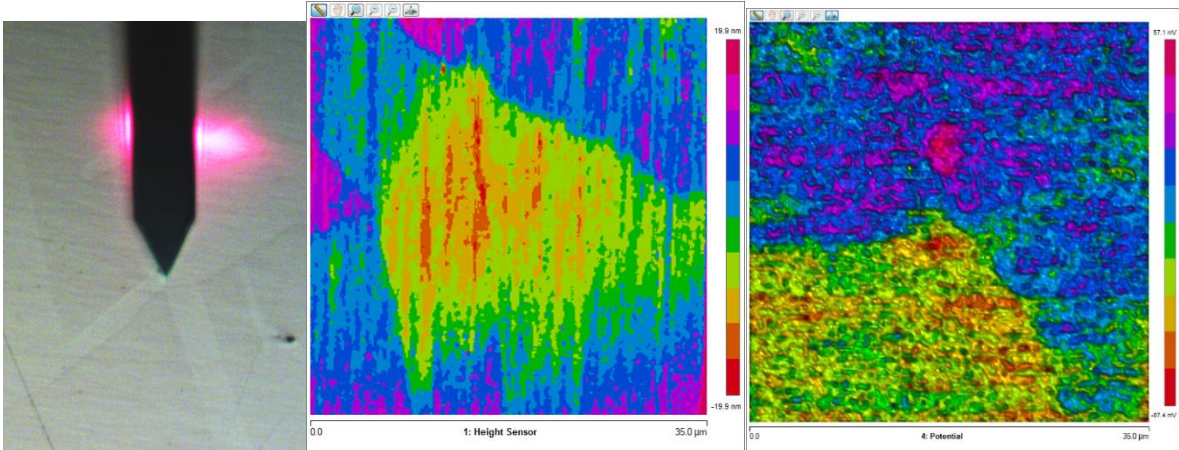


**Figure 21.** Photo (left), topograph (middle) and Volta potential (right) maps of the non-exposed sample, showing small variations (Z-scale) in the height and Volta potential related to the Cu grains.

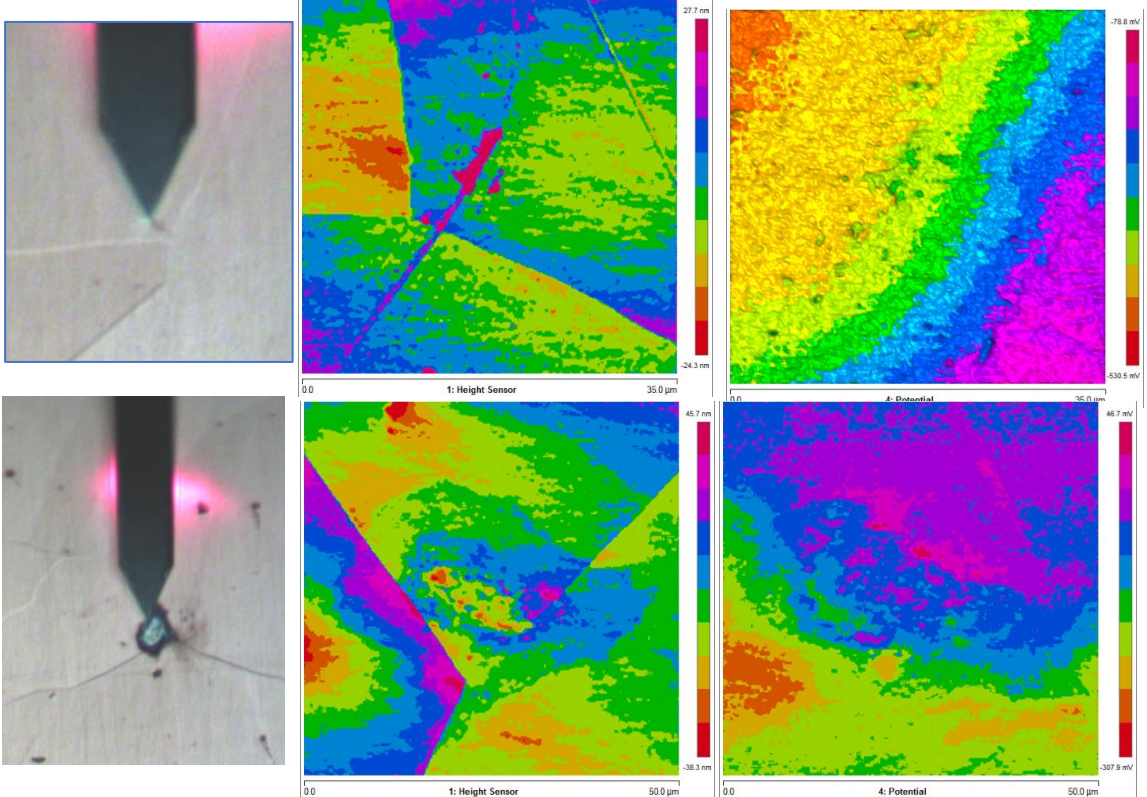


**Figure 22.** Photos (left), topograph (middle) and Volta potential (right) maps of the pre-oxidized sample, showing large variations (Z-scale) in the height and Volta potential, related to the differences in the oxide film on Cu grains. There are more defect sites on the surface, as seen in the bottom line photo and images.

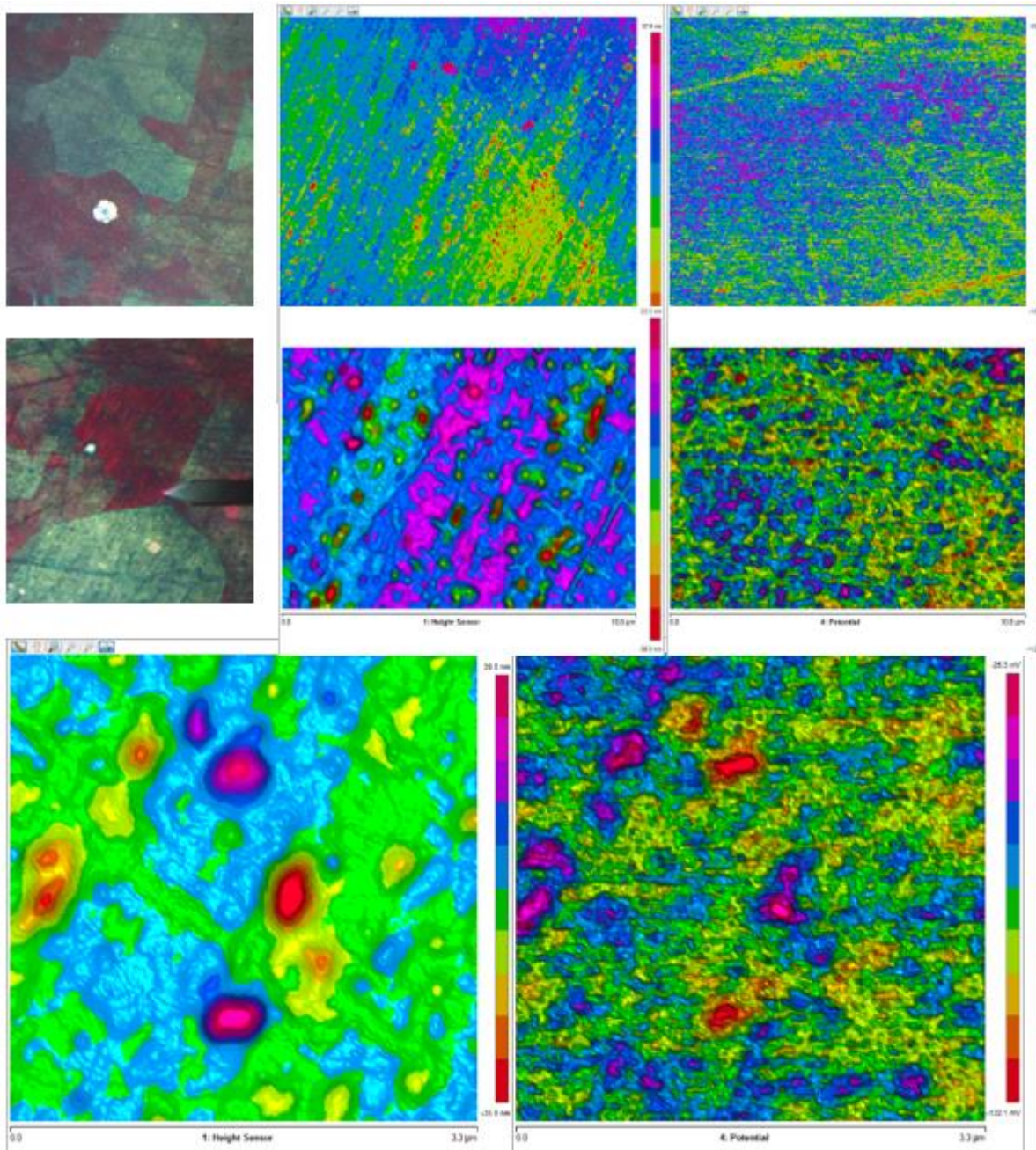


**Figure 23.** Photos (left), topograph (middle) and Volta potential (right) maps of the sample exposed to the ground water containing 32 mg/l sulphide, showing large variations (Z-scale) in the height and Volta potential. The zoomed-view (middle-line and bottom-line images) show the heterogeneous corrosion products on Cu surface, and nodular-type particles in the precipitate surface layer.

### 4.3 Additional experimental tests

#### 4.3.1. Glass corrosion related to experimental test

The additional glass corrosion tests were conducted to study the possible reactions between the test solutions and laboratory glass bottle materials. The 320 and 640 mg/L sulphide solutions were prepared similarly than for corrosion tests. Water samples were collected for analysis from the solutions right after preparation and after 42 days in glass bottles. For glass bottle A type,

only 320 mg/L solution was tested, whereas for bottle B type both 320 and 640 mg/L solutions were tested. Water analysis was performed as described in section 3.3.4.

The results of solution analysis are shown in Table 4. As seen, the analyzed sulphide contents of the solution are all lower than the targeted sulphide values of 320 and 640 mg/L. Especially in the initial waters that may be linked to the technical aspects, because these samples were stored longer in plastic bottles that are used prior the water analysis as part of procedure by analysis provider. The relation of measured  $S^{2-}$  levels between 320 mg/L and 640 mg/L samples is however, quite constant so that the 640 mg/L samples have near two-times higher measured  $S^{2-}$  than 320 mg/L samples. The glass-corrosion related components boron and silicon clearly were found in higher concentrations than the simulated groundwater has. Compared to initial concentration of boron in 320 mg/L solution 1910  $\mu\text{g/L}$  the analyzed value after 42 days in bottle A was 6060  $\mu\text{g/L}$  and in bottle B 5330  $\mu\text{g/L}$ . These concentrations are even higher than those found in first 4-months tests in 2019, that raised the suspicion of the possible reaction between the solution and glass. In case of silicon, the concentration in both 320 mg/L bottles elevated during the exposure so that compared to initial calculated value of 3 mg/L of silicon in simulated groundwater, the measured concentrations were 28.9 mg/L for type A and 27.4 mg/L for type B glass bottle, were evidently higher. Silicon concentration in 2019 was measured only in the part of soluble silicon, whereas here, the total silicon concentration is speculated, because the part of soluble silicon is above detection limit only in 640 mg/L sample. Therefore, comparison to older results is challenging. The solution collected from bottle B filled with 640 mg/L also showed increased concentrations of boron and silicon, which were slightly lower than those measured from 320 mg/L solutions. Thereby, it is evident that the solution used in our studies leaches boron and silicon from the glass vessels. The difference between two tested glass bottles types is minor.

**Table 4.** Water chemistries on the tested solutions of glass corrosion test. Initial refers to solution that has analyzed right after preparation. Other solutions are collected from glass bottles after 42 days. Calculated constituents of simulated groundwater are presented as reference. The most interesting components related to glass corrosion marked in red.

Component	Unit	320 mg/L initial	320 mg/L VWR	320 mg/L Duran	640 mg/L initial	640 mg/L Duran	Simulated groundwater (calculated)	Comment
pH		10.4	10.2	10.2	11.5	11.6		increases with S
carbonates (CO <sub>3</sub> <sup>2-</sup> )	mg/L	262	67.2	50.7		622		unclear
hydrogen sulphide	mg/L	92.1	172	132	199	330		increases with time
sulphide (S <sup>2-</sup> )	mg/L	86.6	162	124	187	311		
acidity, pH 8.3	mmol/L	<0.150	<0.150	<0.150	not analyzed	<0.150		stable
hydrocarbonates (HCO <sub>3</sub> <sup>-</sup> )	mg/L	510	688	435		822	13.7	
carbon dioxide, all	mg/L	560	546	351		1050		
acidity, pH 4.5	mmol/L	<0.150	<0.150	<0.150		<0.150		
carbon dioxide, free	mg/L	0.00	0.00	0.00		0.00		
aggressive carbon dioxide	mg/L	0.00	0.00	0.00		0.00		
alkalinity pH 4.5	mmol/L	17.1	13.5	8.82		34.2		decreasing
alkalinity pH 8.3	mmol/L	4.36	1.12	0.845		10.4		decreasing
Soluble metals:								
B	µg/L	1910	6060	5330		4920	1100	increasing
Cu	µg/L	<20.0	<20.0	<20.0		<20.0		
K	µg/L	110000	111000	121000		120000	54700	Higher than calculated
Mg	µg/L	33800	25400	35800		71.7	100000	
Si	mg/L	<0.200	<0.200	<0.200		9.31	3.1	
Total, Si	mg/L	<6.00	28.9	27.4		19.4		

In conclusion, a lot of uncertainties are related to the water chemistry. Some of them are related to technical aspects and errors that may still be decreased by continuous improvement of laboratory working procedures. Some errors may be linked also to uncertainty of the analytical methods. At the same time, the solution chemistry should be known to understand the chemical processes in our test vessels.

#### 4.3.2 Microstructure of copper samples used

The microstructure of copper samples was studied with optical microscope, to provide supporting information for HEXRD studies. Grain structure representing three different faces of the studied sample are shown in Figures 24-26. Direction 1 corresponds to the large surface of the sheet samples and directions 2 and 3 the side surfaces.



**Figure 24.** Optical micrograph of the etched copper sample, direction 1 (main surface to be studied).

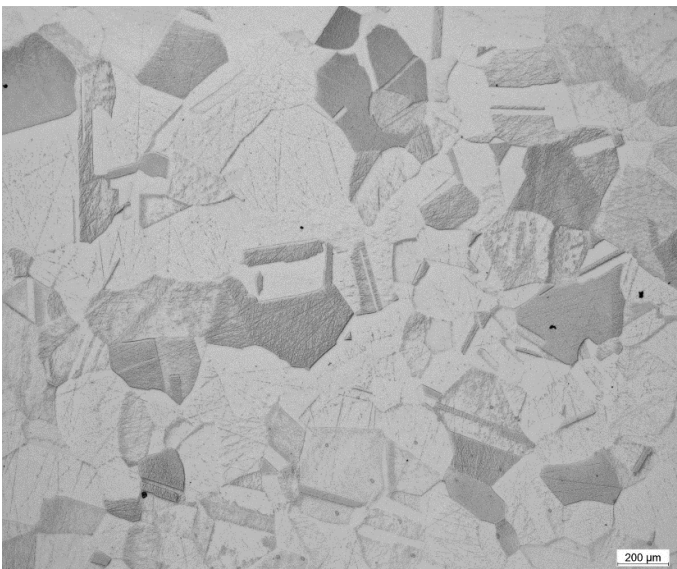


**Figure 25.** Optical micrograph of the etched copper sample, direction 2.

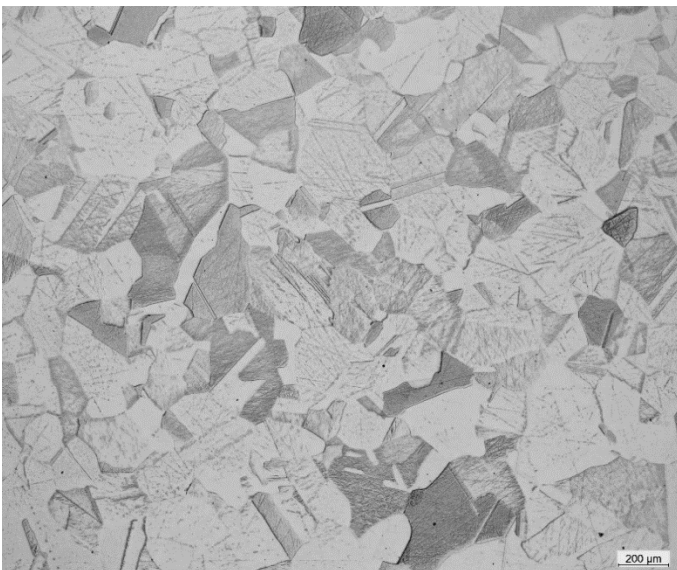


**Figure 26.** Optical micrograph of the etched copper sample, direction 3.

## 5. Summary and conclusions

In the second year of the COCOS project, the work aiming to characterise the sulphide exposed OFP-copper samples continued. After finishing the 4-month experiment in late 2019, work in 2020 was aimed to find suitable and sensitive characterisation methods to reveal the surface structures and possible sulphide-related films and deposits. A lot of efforts were made to ensure reliable and relevant long, 8-9 -month exposure tests, based on the results and the experience learned from the 4-month tests.

The detailed analysis of the sulphide layers formed during the exposure to sulphide containing simulated groundwater is challenging, since both oxides and hydroxides, and different sulphide or sulphate compounds may be formed on the copper surface. The observations from the electrochemical measurements are well supported by the characterization of sample surfaces with, e.g., SEM and EDS. Sulphur-rich precipitated layers were detected, but oxygen leakages may have distorted some of the results. Improved measurement systems to avoid oxygen leakages are used in on-going exposures.

Most importantly, HEXRD studies revealed significant lattice deformation extending several hundreds of micrometers into the bulk. Only hydrogen infusion can explain the measured lattice changes. This is an indication of H-induced initiation on microcracking in the sulphide containing environment. The DFT calculations provided an atomistic understanding of the adsorption and dissociation of sulphide species, the hydrogen infusion and hydrogen-induced lattice dilation in the copper material. As an overall implication the results clearly demonstrate the risk for H-induced stress corrosion cracking of Cu as canister material during long-term storage of nuclear fuel when exposed to sulfide-containing ground water.

A longer experiment (9 months) with increased technical knowledge of the experimental parameters and improved measurement systems was initiated in 2020. In this experiment, varying amount of sulphide additions were used (0-320 mg/L) and copper samples were exposed in both ground/polished and pre-oxidized states. This time, also intermitted additions of sulphide are done to study the effect of uneven sulphide content during the exposure period. The 9-month experiment is currently on-going and will be finalized in spring 2021. Again, a combination of material characterisation methods will be implemented allowing more detailed characterisation of surface related sulfide films and deposits. The work in the project continues and the last long-term measurements will be conducted and finally, all the gained information will be discussed and concluded in the final report.

### Acknowledgments

NKS conveys its gratitude to all organizations and persons who by means of financial support or contributions in kind have made the work presented in this report possible.

Thomas Ohlgschläger from VTT is acknowledged for the consultation in water chemistry expertise. Taru Lehtikuusi, Tuomo Kinnunen, Seija Kivi and Mervi Somervuori are gratefully acknowledged for their assistance with the experiments at VTT. Vuokko Heino, Antti Pasanen and Kati Salonen are acknowledged for their work with the X-ray diffraction experiment at VTT.

We acknowledge PETRA III at DESY in Germany for providing the access to the beamline P21.2 for the synchrotron HEXRD measurement, Diamond Light Source in UK for the access

to the beamline I07 for the synchrotron GIXRD measurement. Moreover, we thank the Swedish National Infrastructure for Computing (SNIC) for providing the Swedish super-computing resource that enabled the DFT calculations.

### Disclaimer

The views expressed in this document remain the responsibility of the author(s) and do not necessarily reflect those of NKS. In particular, neither NKS nor any other organisation or body supporting NKS activities can be held responsible for the material presented in this report.

### 7. References

- Chen, J., Qin, Z., and Shoesmith, D. W. (2011). Long-term corrosion of copper in a dilute anaerobic sulfide solution. *Electrochim. Acta* 56, 7854–7861. doi:10.1016/j.electacta.2011.04.086.
- Hall, D. S., Behazin, M., Jeffrey Binns, W., and Keech, P. G. (2021). An evaluation of corrosion processes affecting copper-coated nuclear waste containers in a deep geological repository. *Prog. Mater. Sci.* 118, 100766. doi:10.1016/j.pmatsci.2020.100766.
- Huttunen-Saarivirta, E., Ghanbari, E., Mao, F., Rajala, P., Carpen, L., and Macdonald, D. D. (2018). Kinetic Properties of the Passive Film on Copper in the Presence of Sulfate-Reducing Bacteria. *J. Electrochem. Soc.* 165, C450–C460. doi:10.1149/2.007189jes.
- Huttunen-Saarivirta, E., Rajala, P., Bomberg, M., and Carpen, L. (2017). Corrosion of copper in oxygen-deficient groundwater with and without deep bedrock micro-organisms: Characterisation of microbial communities and surface processes. *Appl. Surf. Sci.* 396, 1044–1057. doi:10.1016/j.apsusc.2016.11.086.
- Isotahdon, E., Carpen, L., and Rajala, P. (2019). Corrosion of copper in geological repository for nuclear waste - The effect of oxic phase on the corrosion behaviour of copper in anoxic environment. in *Eurocorr2019*.
- King, F., Lilja, C., Pedersen, K., and Pitkanen, P. (2010). *An update of the state-of-the-art report on the corrosion of copper under expected conditions in a deep geologic repository*. Svensk Kärnbränslehantering AB.
- King, F., Lilja, C., and Vähänen, M. (2013). Progress in the understanding of the long-term corrosion behaviour of copper canisters. *J. Nucl. Mater.* 438, 228–237. doi:10.1016/j.jnucmat.2013.02.080.
- Kong, D., Dong, C., Xu, A., Man, C., He, C., and Li, X. (2017). Effect of Sulfide Concentration on Copper Corrosion in Anoxic Chloride-Containing Solutions. *J. Mater. Eng. Perform.* 26, 1741–1750. doi:10.1007/s11665-017-2578-x.
- Nuclear Waste State of the Art Report 2011 (2011).
- Ratia, V., Carpen, L., Isotahdon, E., Örneek, C., Zhang, F., and Pan, J. (2020). NKS-434, Corrosion of copper in sulphide containing environment: the role and properties of sulphide films – Annual report 2019.
- Salonen, T., Lamminmäki, T., King, F., and Pastina, B. (2021). Status report of the Finnish spent fuel geologic repository programme and ongoing corrosion studies. *Mater. Corros.* 72, 14–24. doi:10.1002/maco.202011805.
- SKB - Svensk Kärnbränslehantering AB, SKB, and SKB - Svensk Kärnbränslehantering AB (2019). Supplementary information on canister integrity issues. *Skb Tr-19-15*, 135. Available at: [www.skb.se](http://www.skb.se).

---

Title	Corrosion of copper in sulphide containing environment: the role and properties of sulphide films - Annual report 2020
Author(s)	Elisa Isotahdon <sup>1</sup> , Vilma Ratia <sup>1</sup> , Pauliina Rajala <sup>1</sup> , Leena Carpén <sup>1</sup> , Cem Örneke <sup>2</sup> , Fan Zhang <sup>2</sup> , Jinshan Pan <sup>2</sup>
Affiliation(s)	<sup>1</sup> VTT Technical Research Centre of Finland Ltd., Espoo, Finland <sup>2</sup> KTH Royal Institute of Technology, Stockholm, Sweden
ISBN	978-87-7893-539-7
Date	April 2021
Project	NKS-R / COCOS
No. of pages	35
No. of tables	4
No. of illustrations	26
No. of references	12

**Abstract**  
max. 2000 characters

In COCOS project, the role and properties of sulphide films on copper surface are studied. OFP-copper samples were exposed to sulfide-containing anoxic simulated groundwater for different durations. In 2020, the second year of the COCOS project, the work continued with characterization of previously exposed OFP-copper samples by new techniques. Also, new 9-month long exposure tests were started with sulphide concentrations ranging from 0 to 320 mg/L.

The electrochemical measurements were conducted across the duration of the exposure test. As a result, trends in corrosion behaviour of copper was seen throughout the test. EIS results indicated the formation of the different corrosion product films on sample surfaces exposed. The protective effect of surface layers changes with time of exposure, and the behaviour is influenced by the amount of sulphide in the environment. A distinct and sharp increases in the open circuit potential values of copper samples were observed in some cases during the test. These were more common in environments with low sulphide amount and may be related to time when sulphide has been consumed by chemical reactions. The observation will be further studied in future.

Corrosion rate of samples exposed to 0 mg/L, 32 mg/L and 320 mg/L of sulphide was determined also by measuring mass loss during 4-month test. One interesting finding was that the highest corrosion rates, ca. 0.4 µm/a, were obtained for samples exposed to

sulphide content of 32 mg/L. Sample characterisation showed that the highest mass loss was most likely due to local defects on the samples, not uniform corrosion.

HEXRD studies revealed significant lattice changes as deformation extending several hundreds of micrometers into the bulk. This is attributed to H infusion. The results demonstrate the risk for H-induced stress corrosion cracking of copper as canister material during long-term storage of nuclear fuel when exposed to sulfide-containing groundwater.

The last year of the project is going on at the moment. Longer term experiments have been performed. Further analysis of new samples and data from electrochemical measurements from longer exposures continues. Also, the last new experimental tests will be conducted in 2021.

Key words

corrosion, copper, nuclear waste, sulphide, characterisation